シンポジウム

3. 男性更年期の症状とうつ病との関連

熊野　宏昭　　宮坂菜穂子　　久保木富房

東京大学医学部附属病院心療内科*

要旨：男性更年期外来を受診した初診患者92名を対象に，大うつ病の罹患率と，男性更年期症状を評価する2つの質問紙への回答と大うつ病罹患との関連を調べた。大うつ病の罹患率は，47.8％と非常に高率であった。また，2つの質問紙で評価される症状の大部分は，大うつ病罹患者で有意に高かったが，ほてり，多汗，関節痛，筋痛，手足のしびれ感，髭の伸長の減少，排尿困難，尿失禁など有意差を認めないものもあり，これらが，男性更年期に特異的な症状である可能性が示唆された。

key words　熊本式男性更年期症状調査票，AMS，大うつ病

はじめに

男性更年期における症状とうつ病で出現する症状には，重複するものが多いという臨床的印象がある。そして実際に，高齢者において，うつ状態がテストステロン低下と関連していることを示した報告もある[1,2]。そこで，男性更年期における症状のうち，うつ病との関連が強い症状や，うつ病とは関連の弱い症状を特定することにより，今後の男性更年期に関する質問紙の改善，治療方針の選択，病態生理の研究などに結びつくと考えられる。

何らかの主訴により男性更年期外来を受診する患者には，以下の4つの類型があると想定される。(1) 性腺機能低下，(2) 性腺機能低下＋大うつ病[3,4]，(3) 大うつ病，(4) その他。そこで，(1)＋(4) と (2)＋(3) の間で差のある項目は，大うつ病に伴うものである可能性が高く，逆に差のない項目は，大うつ病とは関係なく男性更年期に特異的な症状である可能性があると予想される。

本研究の目的は以下の2点である。(1) 男性更年期外来におけるうつ病の罹患率を調査すること。(2) 男性更年期における症状のうち，うつ病の有無に関連する症状，うつ病とは関連がなく男性更年期障害に特異的であると考えられる症状を見出すこと。

Ⅰ．対象と方法

全国9施設の泌尿器科男性更年期外来を受診し，研究参加への署名による同意を得た初診患者92名（30～60代）を対象とした。

医師により，年代，向精神薬の服薬およびテストステロン補充療法の有無が聴取され，患者の自

Symptoms evaluated by 2 questionnaires for PADAM and major depressive symptoms

Hiroaki Kumano, Nahoko Miyasaka and Tomifusa Kuboki

Department of Psychosomatic Medicine, Graduate School of Medicine, the University of Tokyo

key words：Kumamoto Male Climacteric Symptoms Inventory, Aging Males' Symptoms scale (AMS), Major depressive disorder

＊文京区本郷7-3-1（03-3815-5411）〒113-8655

表1　大うつ病の判定基準（全5項目以上・うちひとつは1または2）

1 最近2週間以上，毎日のように，ほとんど一日中ずっと憂鬱であったり，沈んだ気持ちでいますか？
2 最近2週間以上，ほとんどのことに興味がなくなっていたり，たいていいつもなら楽しめていたことが楽しめなくなっていますか？
3 毎日のように，食欲が低下，または増加していますか？　または，自分で意識しないうちに，体重が減少，または増加していましたか？
4 毎晩のように，睡眠に問題（たとえば，寝つきが悪い，真夜中に目が覚める，朝早く目覚める，寝すぎてしまうなど）がありますか？
5 毎日のように，普段に比べて話し方や動作が鈍くなったり，またはいらいらしたり，落ち着きがなくなったり，静かに座っていられなくなりますか？
6 毎日のように，疲れを感じたり，または気力がないと感じたりしますか？
7 毎日のように，自分に価値がないと感じたり，自分のことをひどく責めたりしますか？
8 毎日のように，集中したり，決断することが難しいと感じていますか？
9 自分を傷つけたり自殺することや，死んでいればよかったと繰り返し考えますか？

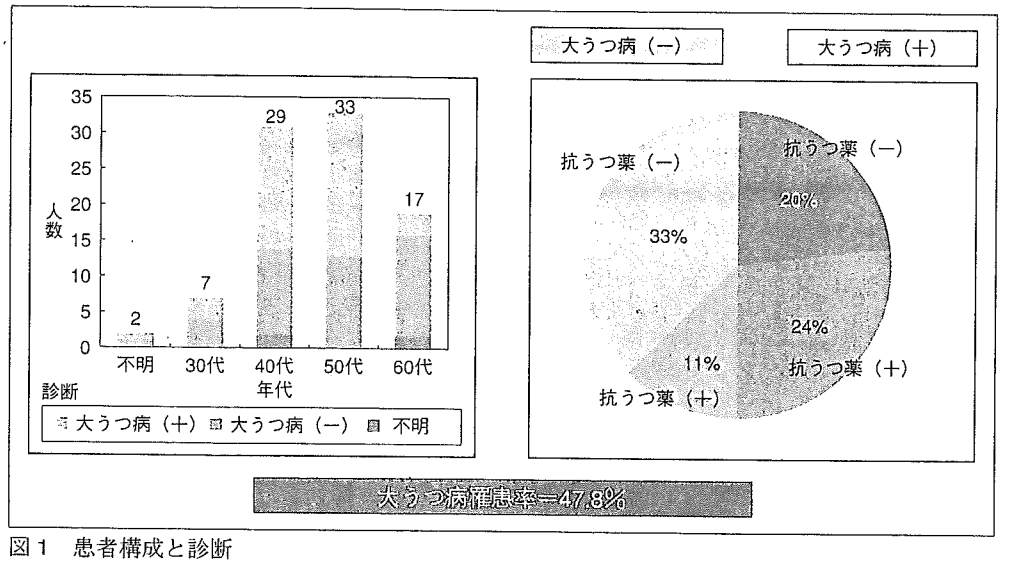

図1　患者構成と診断

己記入により，大うつ病エピソードに関する質問紙（表1：9項目のうち，1または2番目の項目を含む5項目以上を満たす場合に，大うつ病と診断する），熊本式男性更年期症状調査票，Heinemann の Aging Males' Symptoms scale (AMS)[5] の各質問紙が施行された。

最初に，大うつ病の有無を判定した後，それぞれの質問紙の各項目毎に，大うつ病あり・なしの2群間での有意差の有無を，Mann-Whitney の U テストによって検討した。

Ⅱ．結　果

対象者の大うつ病罹患率は，罹患の有無が不明の4名を除いた88名中47.8％であった（図1）。また，質問紙への回答時点で大うつ病の診断は満たさないが，抗うつ薬を服用している患者が，さらに11名（12.5％）存在した。

大うつ病に該当する患者と該当しない患者とで，男性更年期の症状に関する質問紙の得点を比較した結果を，図2，3に示した。熊本式調査票では21項目中13項目に有意差を認め，AMS では17項目中14項目に有意差を認めた。有意差を認めなかったのは，身体症状の一部（ほてり，多汗，関節痛，筋痛，手足のこわばりやしびれ感，髭の伸長の減少）と泌尿器系症状の一部（排尿困難，尿失禁）であった。

Ⅲ．考　察

男性更年期外来の受診患者の約半数が大うつ病に罹患しており，プライマリケア施設での13.9％という報告[6] と比較して，明らかに高率であった。また，特徴的な事実として，60代患者での大うつ病罹患者数は，40～50代と比較して明らかに少ないことも明らかになったが，このことは

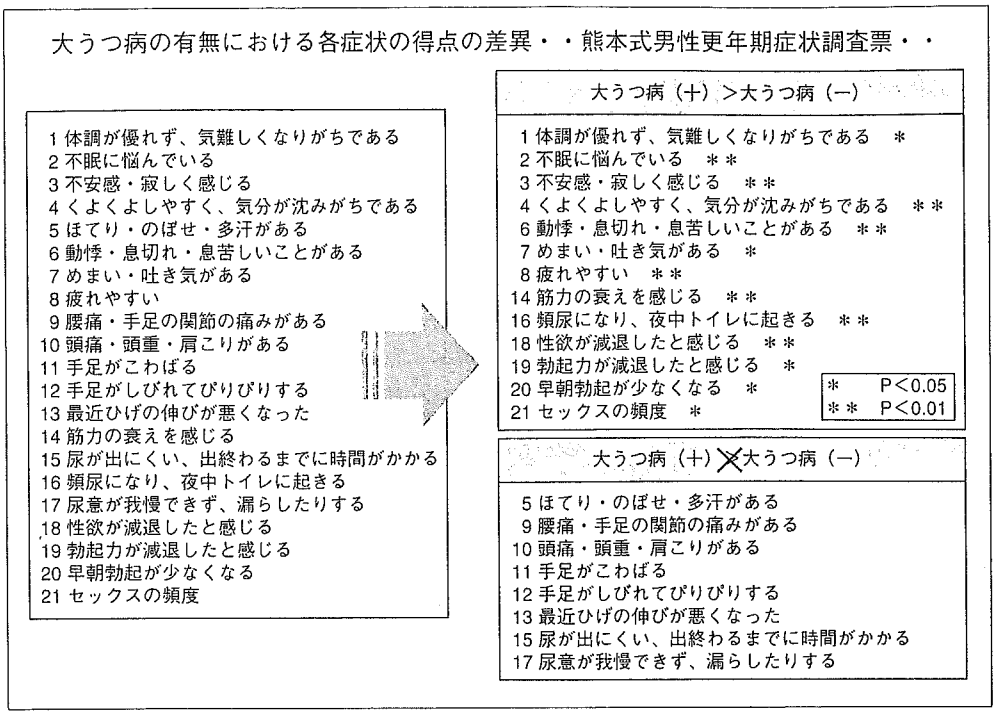

図2　大うつ病の有無でみる男性更年期各症状の得点（1）

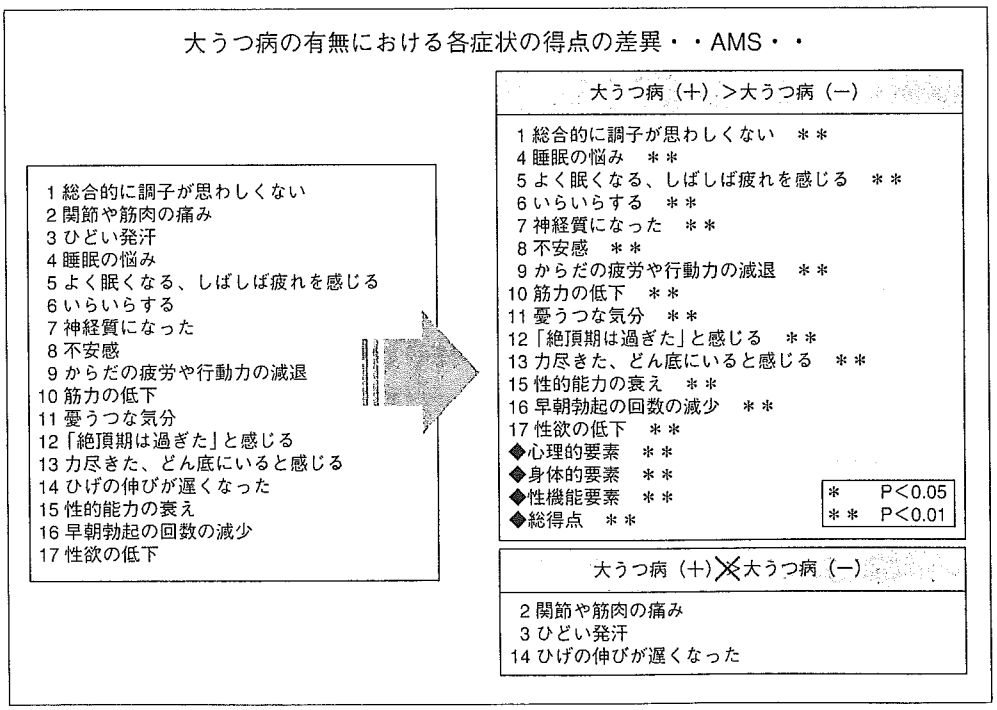

図3　大うつ病の有無でみる男性更年期各症状の得点（2）

60代では，実際に性腺機能低下をきたし身体症状を主訴として受診する者が多いことを示している可能性がある。

本研究では，男性更年期を対象にした2つの質問紙を用いて，それらが評価できる症状とうつ病との関連を検討した。その結果，図4に示したように，うつ病の有無により差異を認めるものが多く，これらは，うつ病に由来する症状を捉えている可能性が高いと考えられた。一方で，身体症状と泌尿器系症状の一部の得点は，うつ病の有無とは関連せず，これらが男性更年期障害に特異的な症状である可能性が示唆された。

今後は，今回検討できなかったテストステロン値と各項目との関連を検討し，男性ホルモンとの関連から男性更年期障害に特異的な項目を明らかにする必要がある。そして，その際には，今回大

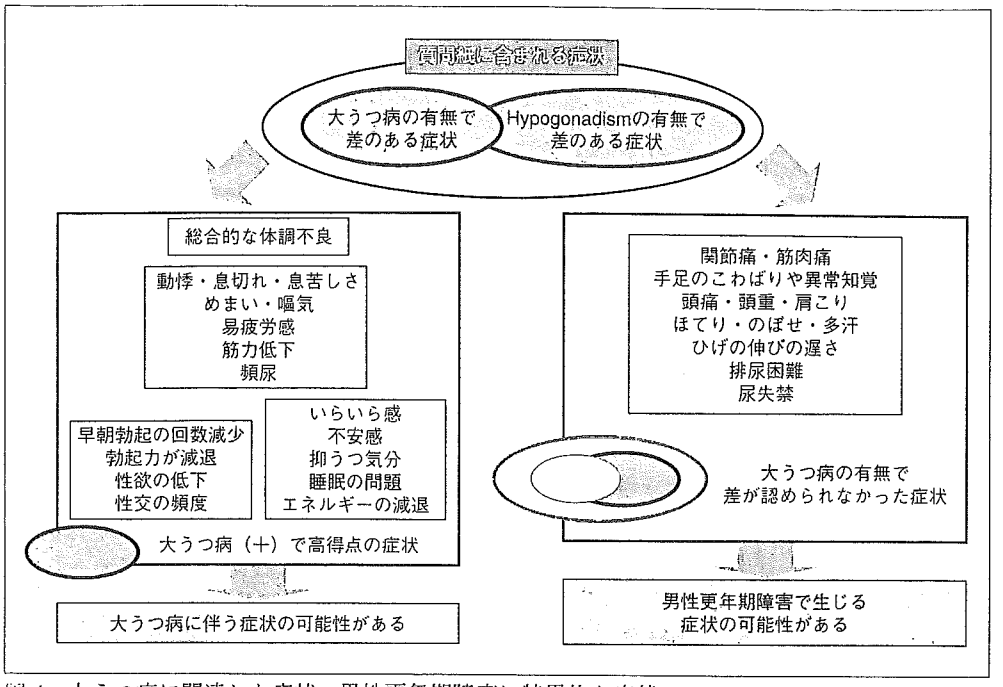

図4　大うつ病に関連した症状・男性更年期障害に特異的な症状

うつ病との関連が示されなかった項目に絞って検討するか，予め大うつ病に罹患している患者を除いて検討することにより，さらに特異性が高く臨床的に有用な項目を明らかにできるであろう。

まとめ

(1) 男性更年期外来の受診患者の約半数が，大うつ病の診断基準に該当した。

(2) 男性更年期を対象にした質問紙で評価した場合，男性更年期外来患者の訴える症状には，大うつ病の有無で得点に有意差のある症状（抑うつ，不安，睡眠障害，動悸，易疲労感，筋力低下，性欲・性機能低下）が多く含まれたが，これらは，大うつ病に由来する症状である可能性が高い。

(3) その一方で，大うつ病の有無で得点に差異のみられない症状（筋痛，関節痛，手足の異常感覚，ひげの伸びの問題，排尿困難，尿失禁）も認められ，これらは男性更年期障害に特異的な症状である可能性があると考えられた。

(4) しかし，これらが実際に男性更年期障害に特異的な症状であるか否かを判断するためには，さらに，テストステロン値との関連の検討を行うことが必要である。またそれと同時に，大うつ病に罹患していない患者を対象に，全項目についてテストステロン値との関連の検討を行うことも次の課題となる。

謝辞

本研究は，以下の先生方（施設の五十音順）の全面的な協力によって実現したものである。心より感謝を申し上げたい。

奥山明彦・辻村晃（大阪大学医学部附属病院泌尿器科），公文裕巳・永井敦（岡山大学医学部附属病院泌尿器科），松田公志（関西医科大学附属病院泌尿器科），横山博美（神田医新クリニック），東原英二・井手久満（杏林大学医学部附属病院泌尿器科），佐藤嘉一（三樹会病院泌尿器科），堀江重郎・丸山修（帝京大学医学部附属病院泌尿器科），石井延久先生・永尾光一（東邦大学医学部附属大森病院泌尿器科），西村泰司（日本医科大学附属病院泌尿器科）。

文　献

1) Barrett-Connor E, Von Muhlen DG and Kritz-Silverstein D: Bioavailable testosterone and depressed mood in older men: the Rancho Bernardo Study. J Clin Endocrinol Metab, **84**, 573-577, 1999.
2) Seidman SN, Araujo AB, Roose SP, et al: Low testosterone levels in elderly men. Am J Psychiatry, **159**, 456-459, 2002.
3) Schweiger U, Deuschle M, Weber B, et al: Testosterone, gonadotropin, and cortisol secretion in male patients with major depression. Psychosom Med, **61**, 292-296, 1999.
4) Carnahan RM and Perry PJ: Depression in aging

men: the role of testosterone. Drugs Aging, **21**, 361-376, 2004.
5) Heinemann LA, Saad F, Zimmermann T, et al: The Aging Males' Symptoms (AMS) scale: Update and compilation of international versions. Health and Quality of Life Outcomes, **1**, 15-19, 2003.
6) Ansseau M, Dierick M, Buntinkx F, et al: High prevalence of mental disorders in primary care. J Affect Disord, **78**, 49-55, 2004.

Available online at www.sciencedirect.com
SCIENCE DIRECT®
Biochemical and Biophysical Research Communications 329 (2005) 1343–1349
BBRC
www.elsevier.com/locate/ybbrc

Overexpression of calreticulin sensitizes SERCA2a to oxidative stress

Yoshito Ihara [a,b,*], Kan Kageyama [a], Takahito Kondo [a]

[a] *Department of Biochemistry and Molecular Biology in Disease, Atomic Bomb Disease Institute, Nagasaki University Graduate School of Biomedical Sciences, Nagasaki 852-8523, Japan*
[b] *CREST, JST Kawaguchi 332-1102, Japan*

Received 9 February 2005

Abstract

Calreticulin (CRT), a Ca^{2+}-binding molecular chaperone in the endoplasmic reticulum, plays a vital role in cardiac physiology and pathology. Oxidative stress is a main cause of myocardiac disorder in the ischemic heart, but the function of CRT under oxidative stress is not fully understood. In this study, the effect of overexpression of CRT on sarcoplasmic/endoplasmic reticulum Ca^{2+}-ATPase (SERCA) 2a under oxidative stress was examined using myocardiac H9c2 cells transfected with the CRT gene. The in vitro activity of SERCA2a and uptake of $^{45}Ca^{2+}$ into isolated microsomes were suppressed by H_2O_2 in CRT-overexpressing cells compared with controls. Moreover, SERCA2a protein was degraded via a proteasome-dependent pathway following the formation of a complex with CRT under the stress with H_2O_2. Thus, we conclude that overexpression of CRT enhances the inactivation and degradation of SERCA2a in the cells under oxidative stress, suggesting some pathophysiological functions of CRT in Ca^{2+} homeostasis of myocardiac disease.

Keywords: Calreticulin; Chaperone; Endoplasmic reticulum; Oxidative stress; SERCA

Calreticulin (CRT) is a Ca^{2+}-binding molecular chaperone expressed in the endoplasmic reticulum (ER) of a wide variety of eukaryote cells [1]. CRT is involved in many biological processes including the regulation of Ca^{2+} homeostasis [2] and intracellular signaling, cell adhesion, gene expression, glycoprotein folding [3,4], and nuclear transport [5]. CRT is well expressed in embryonic rat heart but its expression is suppressed after birth [6]. It has been shown that CRT is essential for cardiac development in mice [7,8]. CRT-deficient embryonic cells showed an impaired nuclear import of nuclear factor of activated T cell (NF-AT3), a transcription factor, indicating that CRT functions in cardiac development as a component of the Ca^{2+}/calcineurin/NF-AT/GATA-4 transcription pathway [7]. On the other hand, CRT transgenic mice suffer a complete heart block and sudden death [9]. The CRT-dependent cardiac block involves an impairment of both the L-type Ca^{2+} channel and gap junction connexins (Cx40 and Cx43). CRT is also over-expressed in rat cardiomyocytes under pressure-overload cardiac hypertrophy, implying some dysfunction of cardiomyocytes related with the overexpression [10]. Furthermore, in cultured myocardiac H9c2 cells, overexpression of CRT following gene transfection promoted apoptosis during cardiac differentiation [11]. These studies suggest that CRT plays a vital role in myocardiac development and function, though how has not been fully clarified.

Sarcoplasmic/endoplasmic reticulum Ca^{2+}-ATPase (SERCA) is an integral membrane protein of the ER or SR that catalyzes the ATP-dependent transport of Ca^{2+} from the cytosol to the lumen of ER or SR [12]. SERCA in the heart plays a pivotal role in the beating function of the heart. SERCA promotes muscle

* Corresponding author. Fax: +81 95 849 7100.
E-mail address: y-ihara@net.nagasaki-u.ac.jp (Y. Ihara).

0006-291X/$ - see front matter © 2005 Elsevier Inc. All rights reserved.
doi:10.1016/j.bbrc.2005.02.112

relaxation by lowering the cytosolic Ca^{2+} concentration and through active Ca^{2+} transport restores the intracellular Ca^{2+} stores, thus providing Ca^{2+} needed for the next contraction. Decreases in SERCA pump expression and activity have been observed in a variety of pathological conditions of the heart [13]. Oxidative stress with reactive oxygen species generated during ischemia and reperfusion is implied in the mechanism for cardiac damage [14]. SERCA is also known to be sensitive to oxidative stress, such as hydroxyl radical, peroxide, and peroxynitrite [15–17]. Inactivation of SERCA by oxidative stress may be implicated in dysfunction of myocardiac cells under the stress.

In *Xenopus* oocytes, it was reported that CRT inhibits Ca^{2+} oscillation enhanced by SERCA2b through the lectin function of CRT [18–21]. Baker et al. [22] have also reported the functional interaction between CRT and SERCA in cultured HeLa cells. However, the pathophysiological significance of CRT expression levels and SERCA functions in cardiomyocytes under oxidative stress has not been revealed. Here we investigated the biological role of CRT using rat myocardiac H9c2 cells transfected with the CRT gene. We first show that overexpression of CRT enhances the inactivation and degradation of SERCA2a via increased interaction with CRT under oxidative stress.

Materials and methods

Materials. Antibodies against CRT (C-terminal), calnexin (CNX), and BiP/Grp78 were purchased from Stressgen (Victoria, BC, Canada). The goat antibody against CRT (N-terminal) was obtained from Santa Cruz Biotechnology (Santa Cruz, CA). The monoclonal antibody against SERCA2 (clone 2A7-A1) was obtained from Sigma (St. Louis, MO). Peroxidase-conjugated secondary antibodies against IgG of rabbit and mouse were from Dako (Denmark). The other reagents used in the study were all of high grade, from Sigma or Wako Pure Chemicals (Osaka, Japan).

Cell lines and culture. H9c2 cells, a clonal line derived from embryonic rat heart, were obtained from American Type Culture Collection (CRL-1446). H9c2 cells which had been transfected with the expression vector for mouse CRT cDNA have been described previously [11]. A cell line (CRT-S8) expressing high level of CRT protein was used in the study. A 0.6-kbp restriction fragment with *Eco*RI, containing the translation initiation site, was cut out from the vector pcDNA3.1/mCRT [11] and inserted in the reverse orientation in pcDNA3.1 (Invitrogen) to obtain an antisense CRT. The antisense cDNA expression vector was also transfected into H9c2 cells to establish a cell line (CRT-AS) in which the expression of CRT was suppressed. Cells were cultured in Dulbecco's modified Eagle's medium, supplemented with 10% fetal calf serum under a humidified atmosphere of 95% air and 5% CO_2 at 37 °C. To induce oxidative stress, cells were cultured with the medium containing different concentrations of H_2O_2.

Immunoprecipitation and immunoblot analysis. Cultured cells were harvested and lysed in lysis buffer [20 mM Tris–HCl (pH 7.2), 130 mM NaCl, and 1% NP-40 including protease inhibitors (20 μM APMSF, 50 μM pepstatin, and 50 μM leupeptin)]. Cell lysates normalized for protein levels were immunoprecipitated using the primary antibodies. After preclearing, the cell lysates were incubated with the primary antibodies at 4 °C for 2 h followed by another 1 h with protein G–Sepharose beads (Amersham Biosciences). For immunoblot analysis, proteins were eluted from the beads by boiling with SDS–dye solution after a wash with the lysis buffer. Protein samples were electrophoresed on 7.5 or 10% SDS–polyacrylamide gels under reducing conditions and then transferred to nitrocellulose membrane as described before [23].

The membrane was blocked with 5% skim milk in TBS [10 mM Tris–HCl (pH 7.5) and 150 mM NaCl] and then incubated at 4 °C overnight with the primary antibody in TBS containing 0.05% Tween 20. The blots were coupled with the peroxidase-conjugated secondary antibodies, washed, and then developed using the ECL chemiluminescence detection kit (Amersham Biosciences) according to the manufacturer's instructions.

Assays of Ca^{2+}-ATPase and Ca^{2+} uptake in the microsomes. For the preparation of microsome, cultured cells were homogenized with homogenization buffer [10 mM Hepes (pH 7.4), 150 mM KCl, 250 mM sucrose, and protease inhibitors]. Homogenates were centrifuged at 1000*g* for 20 min at 4 °C, and then the supernatant was centrifuged at 10,000*g* for 20 min at 4 °C. Supernatants were recovered and ultracentrifuged at 105,000*g* for 60 min at 4 °C. The pellet was resuspended in the homogenization buffer and centrifuged again for 60 min. The final pellet was suspended in the homogenization buffer to obtain a protein concentration of 0.5 mg/ml and stored as a small aliquot at −80 °C. The microsomes were incubated with different concentrations of H_2O_2 for 30 min at 37 °C, and then ATPase and Ca^{2+} uptake activities were determined. Ca^{2+}-dependent ATPase activities were determined spectrophotometrically for untreated and H_2O_2-treated microsomes according to the methods described by Favero et al. [24]. Assays were conducted at 22 °C with 80 μg of microsomal protein in 1 ml of the assay buffer [20 mM Hepes (pH 7.0), 100 mM KCl, 1 mM $MgCl_2$, 1 mM EGTA, 3 mM NADH, 1 mM phosphoenolpyruvate, lactate dehydrogenase (5 U), pyruvate kinase (5 U), and 0.5 mM Mg-ATP]. At first, Ca^{2+}-independent (Mg^{2+}-dependent) ATPase activity was initiated by the addition of the microsome sample to the cuvette, and the change of absorbance at 340 nm was monitored for 2 min. Then, Ca^{2+}-dependent ATPase activity was measured by adding $CaCl_2$ to a final concentration of 10 μM, and again the change of absorbance was monitored for 3 min. The ATPase activity was evaluated from the falling rate of NADH absorbance at 340 nm. Ca^{2+} uptake was measured radiometrically using the Millipore filtration technique as described previously [25] with a slight modification. Assays were conducted on ice with 80 μg of microsomal protein in 90 μl Ca^{2+} uptake buffer consisting of 10 mM Hepes (pH 7.4), 150 mM KCl, 250 mM sucrose, 10 μM ATP, and 1 μCi $^{45}CaCl_2$. The aliquots were incubated on ice for 5 min, and the reaction was terminated by adding 20 μl of 50 mM EGTA and 125 mM $MgCl_2$. Aliquots were filtered through a 0.45-μm nitrocellulose filter under vacuum conditions. The filters were rinsed twice with 0.5 ml of washing buffer [10 mM Hepes (pH 7.4), 150 mM KCl, 2 mM EGTA, and 2.5 mM $MgCl_2$]. $^{45}Ca^{2+}$ uptake was calculated by measuring the radioactivity and standardized using protein concentrations. The data are represented as a percentage of untreated controls.

Fluorescence microscopy. Cells (50,000 per ml) were grown on Lab-Tek chamber slides (Nunc) for 24 h. They were fixed with 4% paraformaldehyde in phosphate-buffered saline (PBS; pH 7.2) and permeabilized for 10 min with PBS containing 1% Triton X-100. The cells were then blocked with 1% BSA in PBS, incubated with the antibody for 1 h, and washed with PBS containing 1% BSA. The immunoreactive primary antibodies were visualized with fluorescein isothiocyanate (FITC)-conjugated anti-rabbit immunoglobulins (Cappel) or rhodamine-conjugated anti-mouse immunoglobulins (Dako). After a wash, the stained cells were mounted in the Vectashield medium. A Zeiss Axioskop2 (Carl Zeiss, Jena, Germany), with epi-illumination for fluorescence, was used for the fluorescence microscopic analysis.

Results

Overexpression CRT enhances the inactivation of SERCA2a in vitro under oxidative stress with H_2O_2

Rat myocardiac H9c2 cells were transfected with the sense and antisense CRT gene expression vectors to obtain cell lines overexpressing and underexpressing CRT, respectively. Fig. 1A shows that the expression of CRT increased in the overexpresser (CRT-S8) to approximately 270% of the level in the parental and mock-transfected (control) H9c2 cells. In the underexpresser (CRT-AS), the expression of CRT was decreased to approximately 30% of the control level. The transfection had no apparent effect on the expression of other ER proteins such as CNX and BiP. Under oxidative stress, a variety of cellular proteins are known to be oxidized and inactivated [26]. SERCA2 is one protein highly susceptible to the stress [15–17]. To examine how the expression level of CRT influences the function of SERCA2a under stress due to H_2O_2, the effect of H_2O_2 treatment on SERCA2a activity was examined in vitro using microsomes isolated from control, CRT-overexpressing, and CRT-underexpressing cells. The microsomes were prepared from cells, treated with different concentrations of H_2O_2 (0–200 μM) for 30 min, and then assayed for SERCA activity as described in Materials and methods. As shown in Fig. 1B, the activity was suppressed after 30-min treatment with H_2O_2 in a dose-dependent manner, and the inactivation was enhanced in CRT-overexpressing cells compared to controls, but was suppressed in CRT-underexpressing cells compared to controls. It was also noteworthy that the expression levels of CRT had less influence on the basal level of SERCA activity in the microsomes of untreated cells. To confirm whether the inactivation of SERCA reflects the loss of Ca^{2+} pumping function, $^{45}Ca^{2+}$ uptake into microsomes was also examined in vitro under the conditions. The microsomes were treated for 30 min with H_2O_2 as described above, and then $^{45}Ca^{2+}$ uptake into microsomes was measured as described in Materials and methods. As shown in Fig. 1C, the uptake of $^{45}Ca^{2+}$ was suppressed by H_2O_2 treatment in a dose-dependent manner, and the suppression was enhanced in CRT-overexpressing cells compared with controls, but was suppressed in CRT-underexpressing cells compared

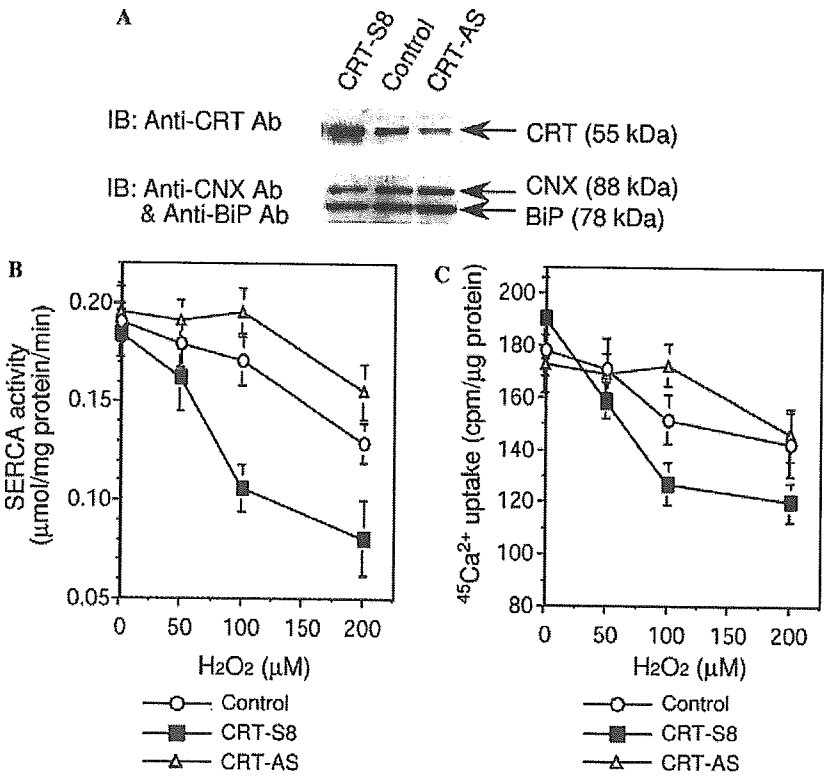

Fig. 1. The expression level of CRT influences the H_2O_2-induced inactivation of SERCA2a and $^{45}Ca^{2+}$ uptake in isolated microsomes in vitro. (A) The expression levels for CRT, CNX, and BiP were estimated in mock-transfected (control), CRT-overexpressing (CRT-S8), and CRT-underexpressing (CRT-AS) cells by immunoblot analysis using specific antibodies as described in Materials and methods. To estimate the effect of H_2O_2 on SERCA2a activity and $^{45}Ca^{2+}$ uptake in isolated microsomes in vitro, microsomes were isolated from control, CRT-overexpressing, and CRT-underexpressing cells as described in Materials and methods. Microsomes were treated with different concentrations of H_2O_2 for 30 min, and then SERCA activity (B) and $^{45}Ca^{2+}$ uptake (C) were measured as described in Materials and methods. Each value represents the mean ± SD of three independent experiments.

with controls. Taken together, overexpression of CRT enhances inactivation of SERCA2a following treatment with H_2O_2, leading to an enhanced suppression of Ca^{2+} uptake into the microsomes. In contrast, suppression of CRT expression prevents the inactivation of SERCA2a following the treatment with H_2O_2.

Overexpression of CRT enhances the degradation of SERCA2a in H9c2 cells under oxidative stress with H_2O_2

To further know the effect of oxidative stress on SERCA2a in CRT-overexpressing cells, the change in the protein level of SERCA2a in whole cells was examined by immunoblot analysis in control and gene-transfected cells during oxidative stress with H_2O_2. Fig. 2A shows

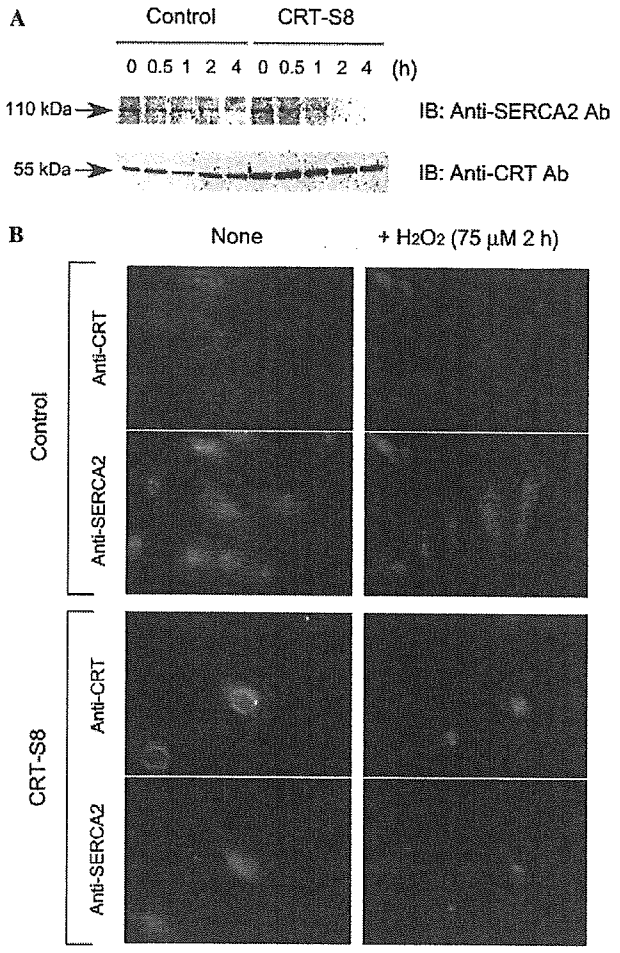

Fig. 2. The expression level of SERCA2a is decreased in CRT-overexpressing H9c2 cells under oxidative stress. (A) Control and CRT gene-transfected (CRT-S8) cells were treated with H_2O_2 (75 μM) for the indicated periods. The expression levels for SERCA2a and CRT were examined by immunoblot analysis using specific antibodies as described in Materials and methods. (B) Control and CRT gene-transfected (CRT-S8) cells were treated with H_2O_2 (75 μM) for 2 h. The intracellular localization of SERCA2a and CRT was examined by immunofluorescence (IF) microscopy using specific antibodies as described in Materials and methods.

that the protein level of SERCA2a apparently decreases 1 h after the treatment with 75 μM H_2O_2 in the gene-transfected cells, with a slight change in control cells. The intracellular localization of SERCA2a was also characterized by immunofluorescence microscopy in control and gene-transfected cells treated with or without 75 μM H_2O_2 for 2 h (Fig. 2B). In control cells, immunoreactivity for SERCA2a showed a perinuclear localization and vesicular pattern, similar to that of CRT, and showed no apparent change after H_2O_2 treatment. On the other hand, CRT was diffusively distributed in the cytoplasm and nucleus after H_2O_2 treatment, although the signal intensity was not diminished by the treatment. In contrast, in the case of gene-transfected cells, damaged cells were round and shrunk with some bleb-like structure, and intracellular compartments seemed destroyed by H_2O_2. Intracellular localization of the signals also showed a diffusive pattern compared to that of untreated cells for both CRT and SERCA2a. Together, in the gene-transfected cells treated with H_2O_2, the structure of intracellular compartments such as ER was apparently destroyed, and the intracellular localization of both CRT and SERCA2a was influenced. Moreover, it was noteworthy that the total cellular level of SERCA2a was apparently decreased in gene-transfected cells during the H_2O_2 treatment, whereas no decrease was seen in that of CRT.

The interaction of CRT with SERCA2a is enhanced in CRT-overexpressing H9c2 cells under oxidative stress with H_2O_2

To investigate whether CRT interacts with SERCA2a under oxidative stress, SERCA2a was immunoprecipitated with the anti-SERCA2 antibody from cell lysates after treatment with H_2O_2 (75 μM) for various periods, and then the immunoprecipitates were subjected to immunoblot analysis using the anti-CRT antibody. As shown in Fig. 3A, CRT was coimmunoprecipitated with the anti-SERCA2 antibody from control cells treated with H_2O_2 for 15 min. The interaction diminished after 30-min treatment with H_2O_2, indicating that CRT transiently interacted with SERCA2a under oxidative stress. On the other hand, CRT was coimmunoprecipitated with anti-SERCA2 antibody from untreated CRT-overexpressing cells. The interaction increased slightly during 60-min treatment with H_2O_2, although the total amount of immunoprecipitated SERCA2a gradually decreased. Conversely, CRT was immunoprecipitated with the specific antibody from cell lysates after treatment with H_2O_2 (75 μM) for various periods, and then the immunoprecipitates were subjected to immunoblot analysis using the anti-SERCA2 antibody. As shown in Fig. 3B, SERCA2a was coimmunoprecipitated with the anti-CRT antibody from control cells treated with H_2O_2 for 15 min. The interaction diminished after 30-min treatment with H_2O_2. This

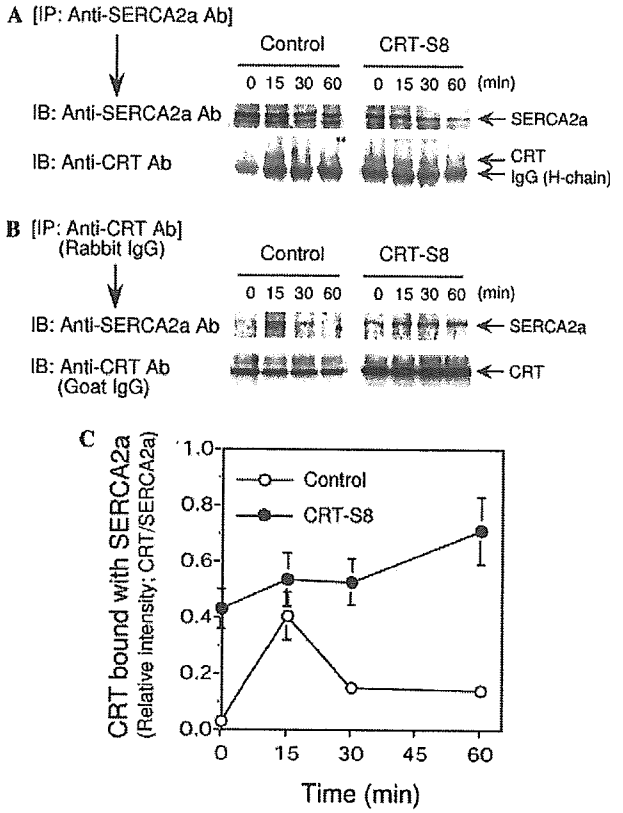

Fig. 3. The interaction between CRT and SERCA2a is increased in CRT-overexpressing H9c2 cells under oxidative stress. Control and gene-transfected (CRT-S8) cells were treated with 75 μM H_2O_2 for the periods indicated. (A) SERCA2a was immunoprecipitated with the specific antibody, then the immunoprecipitates were characterized by SDS–PAGE followed by immunoblot analysis using the anti-SERCA2 and CRT antibodies. (B) CRT was immunoprecipitated with the anti-CRT (C-terminal) antibody, then the immunoprecipitates were characterized by SDS–PAGE followed by immunoblot analysis using the anti-SERCA2 and CRT (N-terminal) antibodies. (C) The protein band intensity for SERCA2a and CRT in A was quantified by densitometry and the relative ratio of CRT bound to SERCA2a was expressed. Each value represents the mean ± SD of four independent experiments.

indicated that SERCA2a transiently interacted with CRT under oxidative stress. In CRT-overexpressing cells, SERCA2a was coimmunoprecipitated with anti-CRT antibody, and the interaction increased slightly during 60-min treatment with H_2O_2. The results were consistent with the data in Fig. 3A. Taken together, these results indicate that CRT transiently interacts with SERCA2a under oxidative stress with H_2O_2, but the interaction is more enhanced and sustained in the CRT-overexpressing cells than controls (Fig. 3C).

SERCA2a is degraded via a proteasome-dependent pathway in CRT-overexpressing H9c2 cells under oxidative stress with H_2O_2

Next to investigate how the H_2O_2-induced degradation of SERCA2a was accelerated in CRT-overexpressing cells, the effect of protease inhibitors on the degradation profile was investigated. In Fig. 4, the effect of lactacystin, a specific inhibitor for proteasomes, on the degradation of SERCA2a was examined by immunoblot analysis in the gene-transfected cells during oxidative stress. In the presence of lactacystin (50 μM), the degradation of SERCA2a was suppressed during oxidative stress. In contrast, leupeptin (120 μM), an inhibitor for lysosomal cysteine and trypsin-like proteases [27], showed no effect on the degradation of SERCA2a during the stress. A lysosomal cysteine protease inhibitor, E64, also showed no effect on the degradation of SERCA2a during the stress (data not shown). Collectively, the results indicate that, in the CRT-overexpressing cells, SERCA2a is degraded by oxidative stress through a proteasome-dependent pathway.

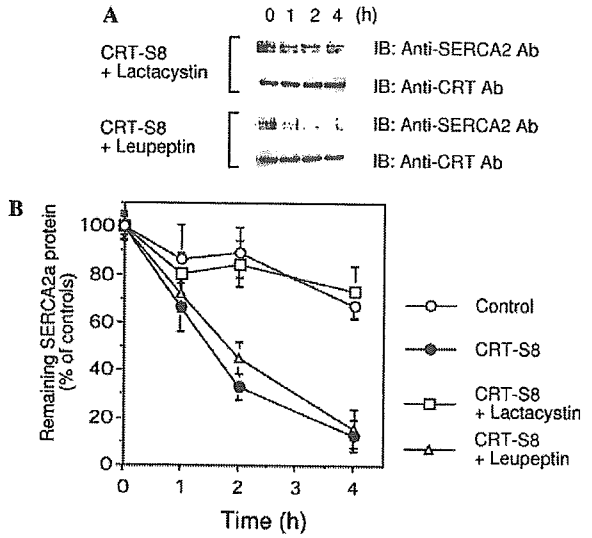

Fig. 4. Overexpression of CRT promotes proteasome-dependent degradation of SERCA2a in H9c2 cells under oxidative stress with H_2O_2. (A) CRT-overexpressing (CRT-S8) cells were treated with 75 μM H_2O_2 for the periods indicated in the presence of lactacystin (50 μM) or leupeptin (120 μM). Degradation of SERCA2a was characterized by immunoblot analysis as described in Fig. 2A. (B) Results of immunoblot analysis with the anti-SERCA2 antibody from three independent experiments for H_2O_2-treated control and gene-transfected (CRT-S8) cells in the presence or absence of lactacystin or leupeptin were quantified by densitometry. The average amount of SERCA2a remaining at each time point was expressed as a percentage of the initial amount of SERCA2a present in the untreated control and gene-transfected cells. Each value represents the mean ± SD of three independent experiments.

Discussion

It is known that the transport of Ca^{2+} by SERCA can be inhibited by superoxide and H_2O_2 in smooth muscle cells [15,16]. It seems that SERCA can be inhibited both by oxidation of its sulfhydryl residues and by a direct attack of oxidants on the ATP-binding site [17]. In the

present study, we focused on SERCA2a function in the CRT-overexpressing cells under oxidative stress, because SERCA is an ER/SR resident protein which is highly susceptible to peroxide stress [16]. We found that in vitro activities of SERCA2a and $^{45}Ca^{2+}$ uptake were both suppressed by H_2O_2 in the microsomes from CRT-overexpressing cells compared with controls. Moreover, the degradation of SERCA2a due to oxidative stress was apparently enhanced in the cells overexpressing CRT. These indicate that the H_2O_2-induced inactivation and degradation of SERCA2a were accelerated by overexpression of CRT, although precise mechanism for acceleration is not known. Actually, CRT transiently interacts with SERCA2a in control cells treated with H_2O_2, suggesting some chaperone function of CRT for SERCA2a under the stress. In the CRT-overexpressing cells, the interaction is rather enhanced during the stress with H_2O_2, and then the trapped SERCA2a undergoes degradation. Although the interaction was detected in the CRT-overexpressing cells, it did not solely enhance the inactivation of SERCA2a under the non-stressed condition. Together, these suggest that, under oxidative stress, prolonged complex formation between unfolded SERCA2a and CRT may be a prerequisite for the inactivation and degradation of SERCA2a.

SERCA is composed of three homologous proteins, SERCA1, SERCA2, and SERCA3 [12]. SERCA2 has two splicing variants, SERCA2a and SERCA2b, which are specifically expressed in cardiac muscle and non-muscle tissues, respectively. Hoch et al. [28] detected a cardiac isotype SERCA2a in H9c2 cells. We also confirmed that isolated SERCA had no N-glycan by immunoblot analysis to determine the sensitivity to endo H and N-glycanase (data not shown), and concluded that the non-glycosylated form of SERCA2a was expressed in H9c2 cells. CRT is known to be a lectin chaperone which mainly functions in the folding and maturation of glycoproteins via monoglucosylated high mannose type N-glycans [2]. However, the interaction between SERCA2a and CRT under the stress may not depend on the oligosaccharides–lectin interaction, which is reported in many cases of chaperone-based interaction with CRT [3]. A peptide-based interaction of CRT with non-glycosylated proteins is reported in protein disulfide isomerase [29], ERp57 [30], and non-glycosylated peptides both in vitro and in vivo [31]. Furthermore, CRT has been shown to discriminate in its binding between native and non-native conformations of non-glycosylated proteins in vitro [32–34]. In this respect, the present study is another in vivo example of a peptide-based interaction of CRT with unfolded non-glycosylated proteins.

In the ER, misfolded proteins are translocated to the cytosol and degraded by the ubiquitin/26S proteasome pathway (ERAD: ER-associated protein degradation) [35]. After forming a complex with CRT and other chaperones, SERCA2a underwent degradation via the proteasome pathway in gene-transfected cells under oxidative stress. In ERAD, misfolded proteins are usually degraded by 26S proteasomes after polyubiquitination [35]. We also investigated the ubiquitination of SERCA2a under stress with H_2O_2, but could not find any increase in the polyubiquitination of immunoprecipitated SERCA2a and associated proteins under the conditions (data not shown). This may not be compatible with the typical ERAD of misfolded proteins of the ER. However, under oxidative stress, oxidized proteins are mainly degraded by 20S proteasomes, not by the ubiquitin/26S proteasome pathway [26]. These results suggest that the H_2O_2-dependent degradation of SERCA2a which was associated with CRT is not simply explained by a typical ERAD process.

We have shown that overexpression of CRT promotes apoptosis during cardiac differentiation in H9c2 cells [11]. In that study, we showed that Akt signaling was suppressed in H9c2 cells overexpressing CRT via an increase in the $[Ca^{2+}]_i$. In addition, we have recently reported that cAMP response element-dependent transcriptional up-regulation of the protein phosphatase 2Acα gene is involved in the inactivation of Akt leading to the enhancement of oxidant-induced apoptosis in H9c2 cells under conditions in which the elevation of $[Ca^{2+}]_i$ is prolonged [36]. These suggest that overexpression of CRT modulates myocardiac functions via the alteration of Ca^{2+} homeostasis in H9c2 cells. In previous reports, overexpression of CRT led to an increase in the intracellular store of Ca^{2+} [2]. CRT also appears to modulate store-operated Ca^{2+} influx [2,37]. However, the precise mechanism behind the altered Ca^{2+} homeostasis caused by overexpression of CRT in H9c2 cells was not clear. For the differentiation of cardiomyocytes, the importance of the intracellular generation of reactive oxygen species is implicated [38]. In this respect, the altered Ca^{2+} homeostasis in the CRT-overexpressing H9c2 cells during the differentiation may be related to a similar mechanism via the regulation of SERCA2a in the cells exposed to oxidative stress, although further investigation is required.

In conclusion, this study indicates that: (1) in myocardiac cells overexpressing CRT, SERCA2a is inactivated by oxidative stress, in accordance with the formation of a complex with CRT; (2) the prolonged formation of the complex promotes degradation of SERCA2a via proteasomes in the CRT-overexpressing cells under oxidative stress. These results suggest that overexpression of CRT modulates the oxidative stress response of myocardiac cells by changing the Ca^{2+} homeostasis via the regulation of SERCA2a.

Acknowledgments

We are grateful to Midori Ikezaki and Akiko Emura for technical assistance. This work was supported in

part by Grants-in-Aid from the Ministry of Education, Science, Sports, Culture and Technology of Japan.

References

[1] M. Michalak, E.F. Corbett, N. Mesaeli, K. Nakamura, M. Opas, Calreticulin: one protein, one gene, many functions, Biochem. J. 344 (1999) 281–292.
[2] M. Michalak, J.M. Robert, Parker, M. Opas, Ca^{2+} signaling and calcium binding chaperones of the endoplasmic reticulum, Cell Calcium 32 (2002) 269–278.
[3] A. Helenius, E.S. Trombetta, D.N. Hebert, J.F. Simons, Calnexin, calreticulin and the folding of glycoproteins, Trends Cell Biol. 7 (1997) 193–200.
[4] S. Johnson, M. Michalak, M. Opas, P. Eggleton, The ins and outs of calreticulin: from the ER lumen to the extracellular space, Trends Cell Biol. 11 (2001) 122–129.
[5] J.M. Holaska, B.E. Black, D.C. Love, J.A. Hanover, J. Leszyk, B.M. Paschal, Calreticulin is a receptor for nuclear export, J. Cell Biol. 152 (2001) 127–140.
[6] K. Imanaka-Yoshida, A. Amitani, S.O. Ioshii, S. Koyabu, T. Yamakado, T. Yoshida, Alteration of expression and distribution of the Ca^{2+}-sorting proteins in endo/sarcoplasmic reticulum during differentiation of rat cardiomyocytes, J. Mol. Cell. Cardiol. 28 (1996) 553–562.
[7] N. Mesaeli, K. Nakamura, E. Zvaritch, P. Dickie, E. Dziak, K.-H. Krause, M. Opas, D.H. MacLennan, M. Michalak, Calreticulin is essential for cardiac development, J. Cell Biol. 144 (1999) 857–868.
[8] F. Rauch, J. Prud'homme, A. Arabian, S. Dedhar, R. St-Arnaud, Heart, brain, and body wall defects in mice lacking calreticulin, Exp. Cell Res. 256 (2000) 105–111.
[9] K. Nakamura, M. Robertson, G. Liu, P. Dickie, K. Nakamura, J.Q. Guo, H.J. Duff, M. Opas, K. Kavanagh, M. Michalak, Complete heart block and sudden death in mice overexpressing calreticulin, J. Clin. Invest. 107 (2001) 1245–1253.
[10] H. Tsutsui, Y. Ishibashi, K. Imanaka-Yoshida, S. Yamamoto, T. Yoshida, M. Sugimachi, Y. Urabe, A. Takeshita, Alteration in sarcoplasmic reticulum calcium-sorting proteins in pressure-overload cardiac hypertrophy, Am. J. Physiol. 272 (1997) H168–H175.
[11] K. Kageyama, Y. Ihara, S. Goto, Y. Urata, G. Toda, K. Yano, T. Kondo, Overexpression of calreticulin modulates protein kinase B/Akt signaling to promote apoptosis during cardiac differentiation of cardiomyoblast H9c2 cells, J. Biol. Chem. 277 (2002) 19255–19264.
[12] F. Wuytack, L. Raeymaekers, L. Missiaen, Molecular physiology of the SERCA and SPCA pumps, Cell Calcium 32 (2002) 279–305.
[13] M. Periasamy, S. Huke, SERCA pump level is a critical determinant of Ca^{2+} homeostasis and cardiac contractility, J. Mol. Cell. Cardiol. 33 (2001) 1053–1063.
[14] N.H. Bishopric, P. Anderka, T. Slepak, K.A. Webster, Molecular mechanisms of apoptosis in the cardiac myocyte, Curr. Opin. Pharmacol. 1 (2001) 141–150.
[15] A.K. Grover, S.E. Samson, Effect of superoxide radical on Ca^{2+} pumps of coronary artery, Am. J. Physiol. 255 (1988) C297–C303.
[16] A.K. Grover, S.E. Samson, V.P. Fomin, Peroxide inactivates calcium pumps in pig coronary artery, Am. J. Physiol. 263 (1992) H537–H543.
[17] G. Ermak, K.J.A. Davies, Calcium and oxidative stress: from cell signaling to cell death, Mol. Immunol. 38 (2002) 713–721.
[18] P. Camacho, J.D. Lechleiter, Calreticulin inhibits repetitive intracellular Ca^{2+} waves, Cell 82 (1995) 765–771.
[19] L.M. John, J.D. Lechleiter, P. Camacho, Differential modulation of SERCA2 isoforms by calreticulin, J. Cell Biol. 142 (1998) 963–973.
[20] H.L. Roderick, J.D. Lechleiter, P. Camacho, Cytosolic phosphorylation of calnexin controls intracellular Ca^{2+} oscillations via an interaction with SERCA2b, J. Cell Biol. 149 (2000) 1235–1247.
[21] Y. Li, P. Camacho, Ca^{2+}-dependent redox modulation of SERCA2b by ERp57, J. Cell Biol. 164 (2004) 35–46.
[22] H.L. Baker, R.J. Errington, S.C. Davies, A.K. Campbell, A mathematical model predicts that calreticulin interacts with the endoplasmic reticulum Ca^{2+}-ATPase, Biophys. J. 82 (2002) 582–590.
[23] Y. Ihara, Y. Sakamoto, M. Mihara, K. Shimizu, N. Taniguchi, Overexpression of N-acetylglucosaminyl transferase III disrupts the tyrosine phosphorylation of Trk with resultant signaling dysfunction in PC12 cells treated with nerve growth factor, J. Biol. Chem. 272 (1997) 9629–9634.
[24] T.G. Favero, A.C. Zable, J.J. Abramson, Hydrogen peroxide stimulates the Ca^{2+} release channel from skeletal muscle sarcoplasmic reticulum, J. Biol. Chem. 270 (1995) 25557–25563.
[25] M. Sumida, Y. Tonomura, Reaction mechanism of the Ca^{2+}-dependent ATPase of sarcoplasmic reticulum from the skeletal muscle. X. Direct evidence for Ca^{2+} translocation coupled with formation of a phosphorylated intermediate, J. Biochem. (Tokyo) 75 (1974) 283–297.
[26] R. Shringarpure, T. Grune, K.J.A. Davies, Protein oxidation and 20S proteasome-dependent proteolysis in mammalian cells, Cell. Mol. Life Sci. 58 (2001) 1442–1450.
[27] V.K. Karaivanova, R.G. Spiro, Effect of proteasome inhibitors on the release into the cytosol of free polymannose oligosaccharides from glycoproteins, Glycobiology 10 (2000) 727–735.
[28] B. Hoch, H. Hasse, W. Schlze, D. Hagemann, I. Morano, E.-G. Krause, P. Karczewski, Differentiation-dependent expression of cardiac δ-CaMK II isoforms, J. Cell. Biochem. 68 (1998) 259–268.
[29] S. Baksh, K. Burns, C. Andrin, M. Michalak, Interaction of calreticulin with protein disulfide isomerase, J. Biol. Chem. 270 (1995) 31338–31344.
[30] E.F. Corbett, K. Oikawa, P. Francois, D.C. Tessier, C. Kay, J.J.M. Bergeron, D.Y. Thomas, K.-H. Krause, M. Michalak, Ca^{2+} regulation of interactions between endoplasmic reticulum chaperones, J. Biol. Chem. 274 (1999) 6203–6211.
[31] S. Basu, P.K. Srivastava, Calreticulin, a peptide-binding chaperone of the endoplasmic reticulum, elicits tumor- and peptide-specific immunity, J. Exp. Med. 189 (1999) 797–802.
[32] C. Svarke, G. Houen, Chaperone properties of calreticulin, Acta Chem. Scand. 52 (1998) 942–949.
[33] Y. Saito, Y. Ihara, M.R. Leach, M.F. Cohen-Doyle, D.B. Williams, Calreticulin functions in vitro as a molecular chaperone for both glycosylated and unglycosylated proteins, EMBO J. 18 (1999) 6718–6729.
[34] A.M. Rizvi, L. Mancino, V. Thammavongsa, R.L. Cantley, M. Raghavan, A polypeptide binding conformation of calreticulin is induced by heat shock, calcium depletion, or by deletion of the C-terminal acid region, Mol. Cell 15 (2004) 913–923.
[35] R.K. Plemper, D.H. Wolf, Retrograde protein translocation: ERADication of secretory proteins in health and disease, Trends Biochem. Sci. 24 (1999) 266–270.
[36] C. Yasuoka, Y. Ihara, S. Ikeda, Y. Miyahara, T. Kondo, S. Kohno, Antiapoptotic activity of Akt is down-regulated by Ca^{2+} in myocardiac H9c2 cells. Evidence of Ca^{2+}-dependent regulation of protein phosphatase 2Ac, J. Biol. Chem. 279 (2004) 51182–51192.
[37] S. Arnaudeau, M. Frieden, K. Nakamura, C. Castelbou, M. Michalak, N. Demaurex, Calreticulin differentially modulates calcium uptake and release in the endoplasmic reticulum and mitochondria, J. Biol. Chem. 277 (2002) 46696–46705.
[38] H. Sauer, G. Rahimi, J. Hescheler, M. Wartenberg, Role of reactive oxygen species and phosphatidylinositol 3-kinase in cardiomyocyte differentiation of embryonic stem cells, FEBS Lett. 476 (2000) 218–223.

Glycobiology vol. 15 no. 4 pp. 383–392, 2005
doi:10.1093/glycob/cwi012
Advance Access publication on November 3, 2004

Increased expression of protein C-mannosylation in the aortic vessels of diabetic Zucker rats

Yoshito Ihara[1,2,3], Shino Manabe[3,4], Munetake Kanda[2,5], Hiroaki Kawano[5], Toshiyuki Nakayama[6], Ichiro Sekine[6], Takahito Kondo[2], and Yukishige Ito[3,4]

[2]Department of Biochemistry and Molecular Biology in Disease, Atomic Bomb Disease Institute, Nagasaki University Graduate School of Biomedical Sciences, 1-12-4 Sakamoto, Nagasaki 852-8523, Japan; [3]CREST, JST Kawaguchi 332-1102, Japan; [4]RIKEN (Institute of Physical and Chemical Research), Saitama 351-0198, Japan; [5]Third Department of Internal Medicine, Nagasaki University Graduate School of Biomedical Sciences, 1-12-4 Sakamoto, Nagasaki 852-8523, Japan; [6]Department of Molecular Pathology, Atomic Bomb Disease Institute, Nagasaki University Graduate School of Biomedical Sciences, 1-12-4 Sakamoto, Nagasaki 852-8523, Japan

Received on October 20, 2004; revised on November 1, 2004; accepted on November 2, 2004

C-Mannosylation is a novel type of glycosylation in proteins. There are several examples of proteins in which the specific motif *Trp*-X-X-Trp is mannosylated at the first Trp to produce C-mannosylated Trp (CMW). Although C-mannosylation modifies Trp-X-X-Trp, predicted to be a functional motif of various integral proteins such as cytokine receptors, the physiological or pathological relevance of C-mannosylation in the cell is still not known. In this study, to characterize C-mannosylation in biological samples, we generated specific polyclonal antibodies against CMW by using a chemically synthesized CMW as an antigen. Using the antibody, we investigated the effect of hyperglycemic conditions on protein C-mannosylation in cultured cells and diabetic Zucker fatty rats. We found that protein C-mannosylation was increased in macrophage-like RAW264.7 cells under hyperglycemic conditions compared to low-glucose conditions. Furthermore, C-mannosylation was increased in the aortic vessel wall of Zucker fatty rats. Thrombospondin-1 was identified as a protein modified with C-mannosylation, and its expression was also increased in the aortic tissues of Zucker fatty rats. These results indicate that C-mannosylation is increased in specific tissues or cell types under hyperglycemic conditions, suggesting a pathological role for the increased C-mannosylation in the development of diabetic complications.

Key words: C-mannosylation/diabetes/hyperglycemia/mannosyltransferase/thrombospondin

Introduction

Glycosylation is a major modification of cellular proteins. Protein-bound glycans are classified by the nature of their linkage to the protein (Spiro, 2002). N-glycan (N-linked oligosaccharide) is a major modified form in which N-acetylglucosamine (GlcNAc) is first bound to Asn via an acidic amide bond. The subsequent processing of sugar chains has been extensively characterized (Kornfeld and Kornfeld, 1985). O-glycan (O-linked oligosaccharide) is another major modified form in which mainly N-acetylgalactosamine is bound to the hydroxyl residue of Ser or Thr in proteins (Schachter and Brockhausen, 1989). The processing of O-glycan has also been well characterized. In addition to O-glycans, other saccharides, such as mannose, fucose, and GlcNAc, attach directly to Ser or Thr via the hydroxyl residue (Spiro, 2002).

C-mannosylation is a novel type of protein glycosylation discovered by Hofsteenge *et al.* (1994). C-mannosylation is unique in that an α-mannose is directly bound to the indole C2 carbon atom of a Trp residue through a C-C bond to produce C-mannosylated Trp (CMW) (Figure 1). C-mannosylation occurs at the first Trp in the consensus amino acid sequence *Trp*-X-X-Trp in proteins. There are several examples of C-mannosylated proteins, including RNase2, interleukin-12, complements (C6, C7, C8a, C8b, and C9), properdin, thrombospondin, F-spondin, the erythropoietin receptor, and mucins (MUC5AC and MUC5B) (De Peredo *et al.*, 2002; Furmanek and Hofsteenge, 2000; Furmanek *et al.*, 2003; Hartmann and Hofsteenge, 2000; Hofsteenge *et al.*, 2001; Perez-Vilar *et al.*, 2004). C-mannosylation is thought to be synthesized by a specific unidentified mannosyltransferase localized in the microsomes (Doucey *et al.*, 1998), suggesting that C-mannosylation is involved in conventional glycosylation through the secretory pathway. This is consistent with the fact that almost all the C-mannosylated proteins found to date are secretory or membrane proteins. On the other hand, monomeric CMW was isolated from human urine (Gutsche *et al.*, 1999; Horiuchi *et al.*, 1994) and marine ascidians (Garcia *et al.*, 2000; Van Wagoner *et al.*, 1999), although the biological significance of the monomeric form is not known. It was reported that monomeric CMW in blood could be a novel biomarker of renal function (Takahira *et al.*, 2001). The functional relevance of glycosylation has been revealed in various cellular events, including cell development, growth, differentiation, and death (Dennis *et al.*, 1999; Haltiwanger and Lowe, 2004; Lowe and Marth, 2003; Varki, 1993). However, the biological significance of C-mannosylation has yet to be fully investigated.

Here we describe the generation of specific antibodies against CMW. We also report the effect of hyperglycemic conditions on protein C-mannosylation in cultured cells and diabetic rat tissues. This is the first report concerning the characterization of protein C-mannosylation in the cell under pathological conditions such as diabetes mellitus.

[1]To whom correspondence should be addressed; e-mail: y-ihara@net.nagasaki-u.ac.jp

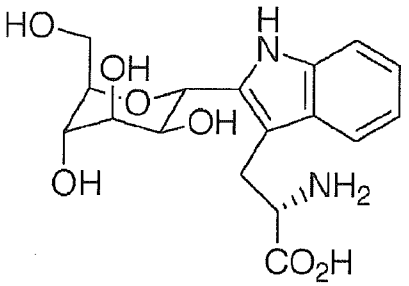

Fig. 1. The chemical structure of C-mannosylated Trp (CMW).

Results

Characterization of antibodies against C-mannosylated Trp

To obtain specific antibodies against CMW (Figure 1), CMW was chemically synthesized as described by Manabe and Ito (1999). Rabbit antibodies against CMW were generated by immunizing CMW conjugated to keyhole limpet heamocyanine (KLH). The antibody was affinity-purified by using a C-mannose-Trp-Ser-Pro-Trp-Cys-conjugated resin as described in *Materials and methods* and was used for the following experiments. To determine whether the antibody recognizes CMW, an enzyme-linked immunosorbent assay (ELISA) was carried out using the CMW conjugated to ovalbumin (Figure 2A). The results showed that the anti-CMW antibody reacted well with the CMW-conjugated ovalbumin but exhibits poor activity toward ovalbumin. The control IgG showed no significant reactivity to either ovalbumin or the CMW-conjugated ovalbumin. In Figure 2B, the anti-CMW antibody was preincubated at room temperature for 30 min with 1 mM glucose, mannose, or CMW; then ELISA was carried out in the presence of each factor. The immunoreactivity of the anti-CMW antibody was significantly suppressed in the presence of CMW but not glucose or mannose. In Figure 3, the reactivity and sensitivity of the antibody were examined by immunoblot analysis using ovalbumin conjugated with or without CMW. The results showed that the antibody reacted well with the CMW-conjugated ovalbumin but exhibited poor activity toward ovalbumin. Furthermore, the immunoreactivity of the anti-CMW antibody was apparently suppressed by CMW but not by glucose or mannose. Together, these results indicate that the anti-CMW antibody specifically reacts with CMW in ELISA and immunoblot analysis.

Characterization of protein C-mannosylation in RAW264.7 cells cultured with low or high glucose concentrations

To investigate whether hyperglycemic conditions affect the level of protein C-mannosylation in cultured cells, mouse macrophage-like RAW264.7 cells were cultured with a low (5.5 mM) or high (30 mM) glucose medium for more than 5 days, and the C-mannosylation was examined immunologically. In Figure 4A, the expression level of CMW was examined by immunoblot analysis using the anti-CMW antibody in the cells cultured with low or high glucose concentrations. The level of C-mannosylation was increased in

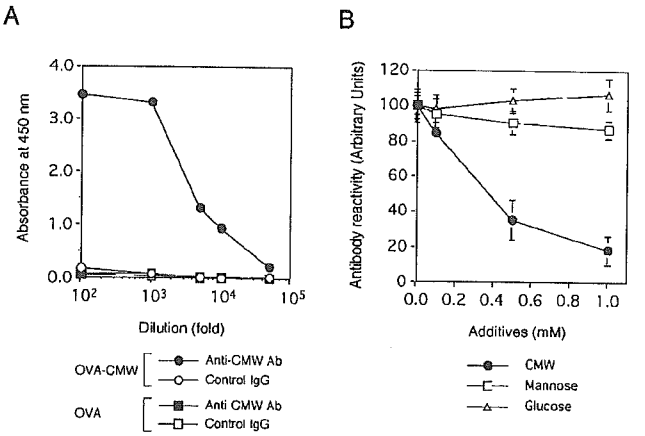

Fig. 2. ELISA for the antibody against CMW. (**A**) ELISA was carried out using 96-well microwell plates coated with CMW-conjugated ovalbumin (OVA) or OVA as described in *Materials and methods*. The primary antibodies (1 mg/ml) were diluted as indicated and used for the assay. The immunoreactivity of the peroxidase-conjugated secondary antibodies was estimated by using TMB one solution. (**B**) ELISA was carried out using 96-well microwell plates coated with CMW-conjugated OVA as described in *Materials and methods*. The anti-CMW antibody (0.1 μg/ml) was incubated in the wells with or without 1 mM glucose, mannose, or CMW, and the immunoreactivity to CMW-conjugated OVA was estimated as described.

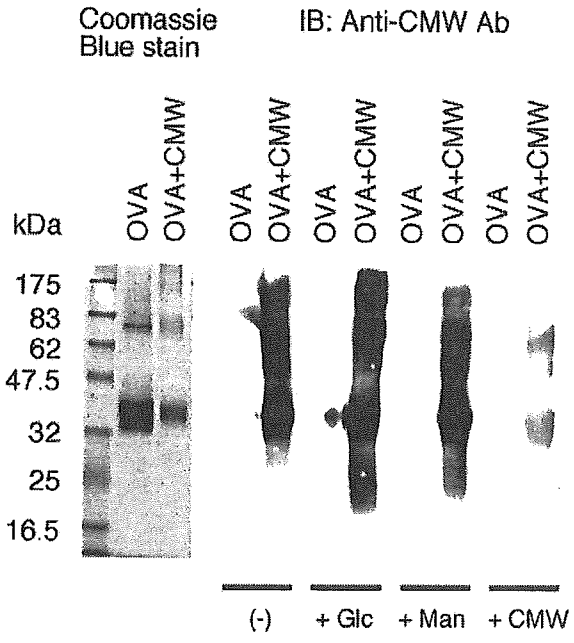

Fig. 3. Immunoblot analysis using the antibody against CMW. Immunoblot analysis using the anti-CMW antibody was carried out as described in *Materials and methods*. Ovalbumin (OVA) and CMW-conjugated OVA were subjected to 10% SDS–PAGE followed by blotting to the nitrocellulose membrane. The blotted membranes were incubated with the anti-CMW antibody in the presence or absence of 1 mM of glucose (Glc), mannose (Man), or CMW. Immunoreactive bands were visualized using peroxidase-conjugated secondary antibodies and the a chemiluminescence detection kit.

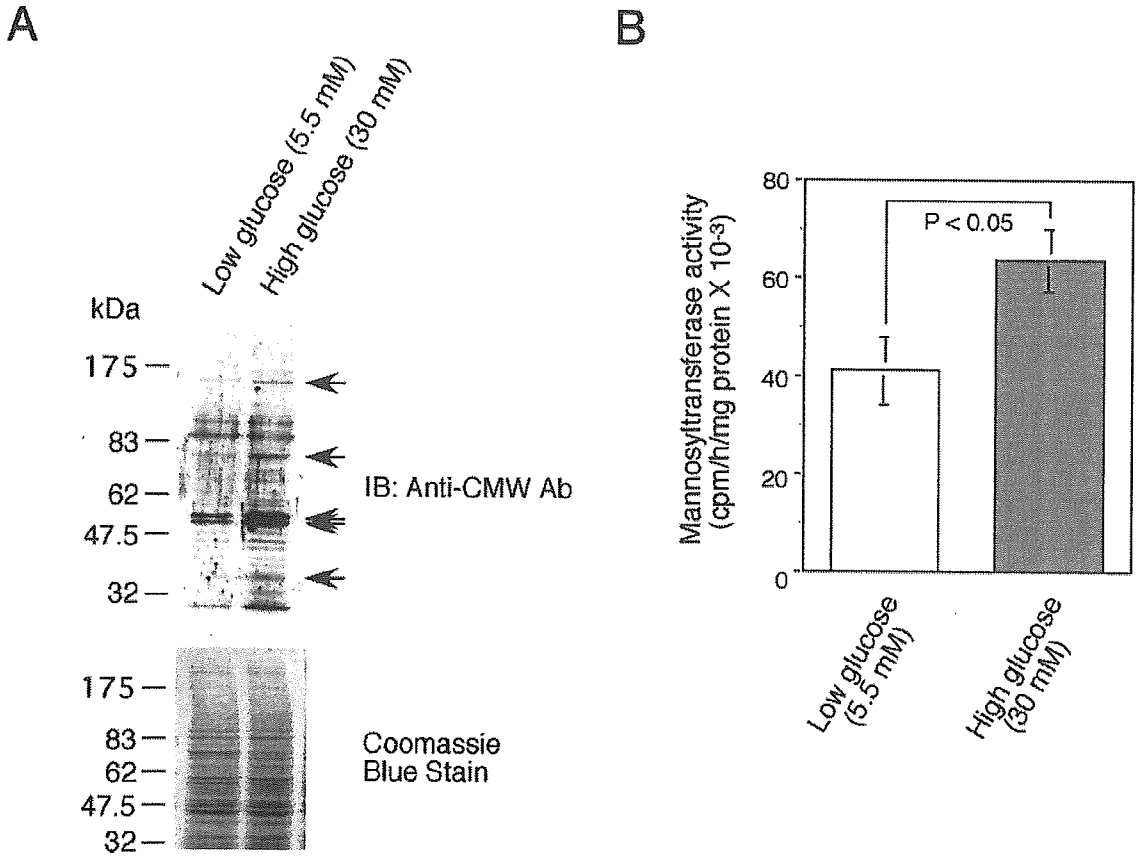

Fig. 4. Effect of hyperglycemic conditions on protein C-mannosylation in RAW264.7 cells. (**A**) Eells were cultured in media with low (5.5 mM) or high (30 mM) glucose concentrations as described in *Materials and methods*. The expression level of CMW was estimated by immunoblot analysis using the anti-CMW antibody as described. The results represent three independent experiments. (**B**) The C-mannosyltransferase activity was assayed with cell homogenates from the cells cultured with low or high glucose concentrations as described. The samples were incubated at 37°C for 4 h with the substrate peptide N-AC-Lys-Pro-Pro-Gln-Phe-Ala-Trp-Ala-Gln-Trp-Phe-Glu-NH_2 and dolichol-P-[6–^{3}H]mannose (0.25 μCi). The reaction was stopped by extraction with chloroform/methanol, and mannosylation of the peptide was estimated by measuring the uptake of radioactivity in the aqueous phase. The data represent the mean ± SD of four independent experiments. The statistical analysis was performed with a paired Student *t*-test.

the hyperglycemic conditions especially in protein bands corresponding to 155, 76, 54, 52, and 35 kDa (arrows).

To investigate the mechanical link between the C-mannosylation and the activity of C-mannosyltransferase which is known to be responsible for the synthesis of C-mannosylated protein, the enzymatic activity was examined in the cell lysates from low- and high-glucose cultures. As shown in Figure 4B, the activity was increased under the hyperglycemic conditions rather than low-glucose conditions. These results suggest that the C-mannosyltransferase activity for CMW was increased in RAW264.7 cells cultured with a high concentration of glucose, resulting in the increased expression of C-mannosylated forms of specific cellular proteins under the hyperglycemic conditions. Next, the intracellular localization of C-mannosylated proteins was visualized in RAW264.7 cells by indirect immunofluorescence microscopy using the anti-CMW antibody (Figure 5). The immunoreactive signals showed a perinuclear vesicular pattern, and the intensity of the signals was enhanced in the cells cultured with high glucose rather than low glucose. To see the secretory vesicles, localization of clathrin heavy chain, a marker for secretory vesicles and the trans-Golgi network (Ihara *et al.*, 2002), was also examined by indirect immunofluorescence microscopy. The immunoreactive signals of clathrin heavy chain showed a very similar localization to those of protein C-mannosylation, suggesting that C-mannosylated proteins might be localized in the secretory pathway of the cell.

Characterization of protein C-mannosylation in tissues of diabetic Zucker rats

To investigate whether hyperglycemia influences C-mannosylation in the tissues of those with diabetes, C-mannosylation was characterized immunologically in the male Zucker diabetic fatty (fa/fa) rat, an animal model of type II diabetes (Zucker and Antoniades, 1972). Nondiabetic Zucker lean (fa/+) rats were used as controls. Twenty-week-old rats were used for the study, because Zucker fatty rats exhibit hyperinsulinemia and hyperlipidemia at 6 weeks and become diabetic from 14 weeks (Coimbra *et al.*, 2000). Blood glucose levels for Zucker fatty, lean, and Sprague Dawley (another control) rats were 343.7 ± 22.5, 140.2 ± 35.0, and 152 ± 18.3 (mg/dl), respectively. Furthermore, blood insulin levels were 12.7 ± 1.5, 1.2 ± 0.4, and 0.9 ± 0.3

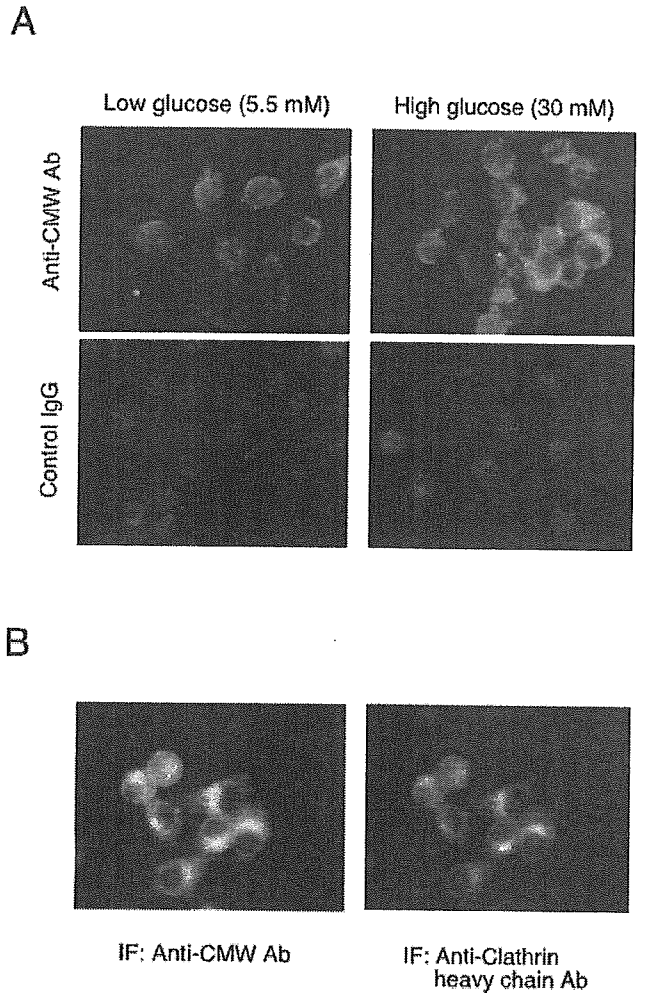

Fig. 5. Indirect immunofluorescence of CMW in RAW264.7 cells. (A) Eells were cultured in media with low or high glucose concentrations as described in Figure 4. The intracellular localization of CMW was examined by indirect immunofluorescence (IF) microscopy using the specific antibody. (B) Cells cultured with the high-glucose medium were simultaneously incubated with both antibodies against CMW (rabbit IgG) and clathrin heavy chain (mouse monoclonal IgG). The intracellular localization of CMW and clathrin heavy chain was then visualized microscopically with FITC-conjugated anti-rabbit IgG and rhodamine-conjugated anti-mouse IgG, respectively.

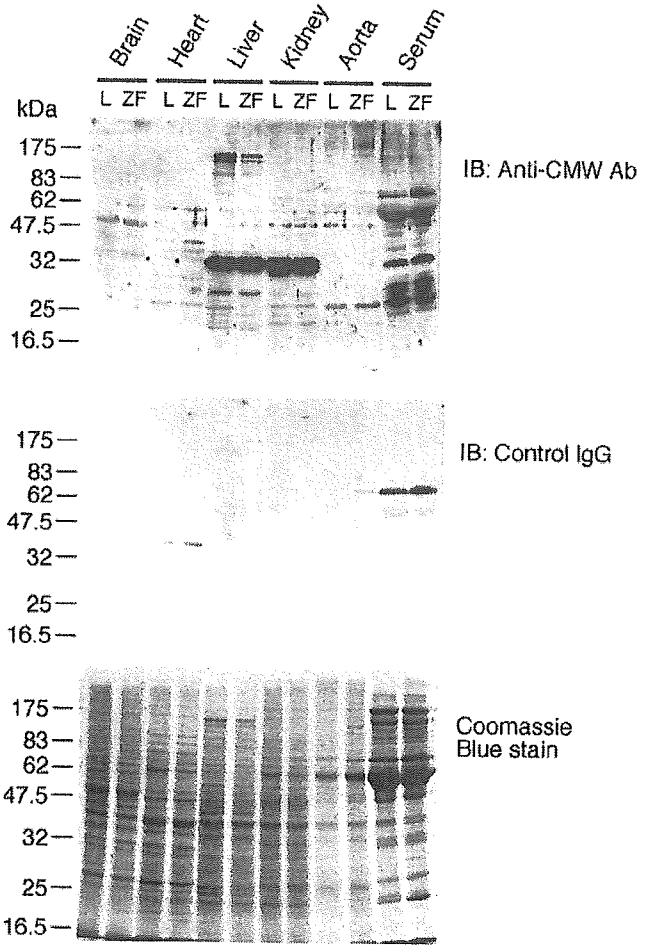

Fig. 6. The level of protein C-mannosylation in several tissues of diabetic Zucker fatty and control lean rats. Samples of tissue homogenates (brain, heart, liver, kidney, and aorta) and serum were prepared from Zucker fatty (ZF) and lean (L) rats as described in *Materials and methods*. The expression of C-mannosylation of protein was examined by immunoblot analysis with the anti-CMW antibody as described. Immunoblotting with control IgG was also performed as a control. The results represent three independent experiments.

(ng/ml), respectively. These results indicated that Zucker fatty rats showed hyperglycemia and hyperinsulinemia at 20 weeks of age, whereas no symptoms were observed in lean and Sprague Dawley rats. This was also consistent with previous results (Coimbra *et al.*, 2000). As shown in Figure 6, the expression of C-mannosylated protein was examined in several tissues by immunoblot analysis using the anti-CMW antibody. In the tissue homogenates from brain, heart, liver, kidney, and serum, no significant difference was seen between Zucker fatty and lean rats in the level of C-mannosylation. In contrast, C-mannosylation was apparently increased in the aorta of Zucker fatty compared to lean rats. These results indicate that hyperglycemia increases the expression of C-mannosylated protein not in all tissues but in specific tissues, such as the aorta.

C-mannosylation is increased in the aortic vessel wall of Zucker fatty rats

To further characterize the expression of C-mannosylated protein in the aorta of Zucker fatty rats, C-mannosylation was examined immunohistochemically in the aortic vessel tissues using the anti-CMW antibody (Figure 7). The tissues were also counterstained with hematoxylin and eosin. In the aorta of Zucker fatty rats, no typical atherosclerotic change was observed compared to that of lean rats. However, the level of C-mannosylation was elevated in vessel walls of Zucker fatty compared to lean rats, and signals were diffusely seen in the intracellular and extracellular parts of whole layers of the vessel.

Recently, Stenina *et al.* (2003) reported that thrombospondin-1 (TSP-1) is induced in the aortic vessel wall of Zucker fatty rats, suggesting a pathogenic contribution of the increased expression of TSP-1 to the atherocsclerotic

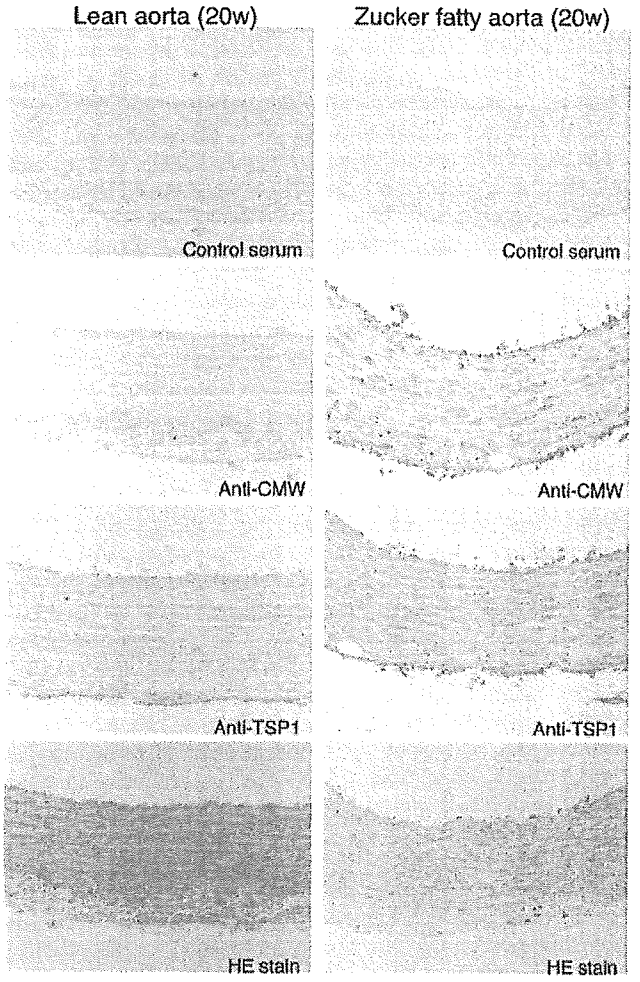

Fig. 7. Immunohistochemistry of CMW in the aortic vessels of diabetic Zucker rats. Paraffin-embeded samples of aortic vessels from Zucker fatty and lean rats (20 weeks old) were sectioned and subjected to indirect immunohistochemical staining using antibodies against CMW and TSP-1. Immunoreactive signals from primary antibodies were visualized with diaminobenzidine chromogenic substrate as described in *Materials and methods*. Sections were counterstained with hematoxylin and eosin.

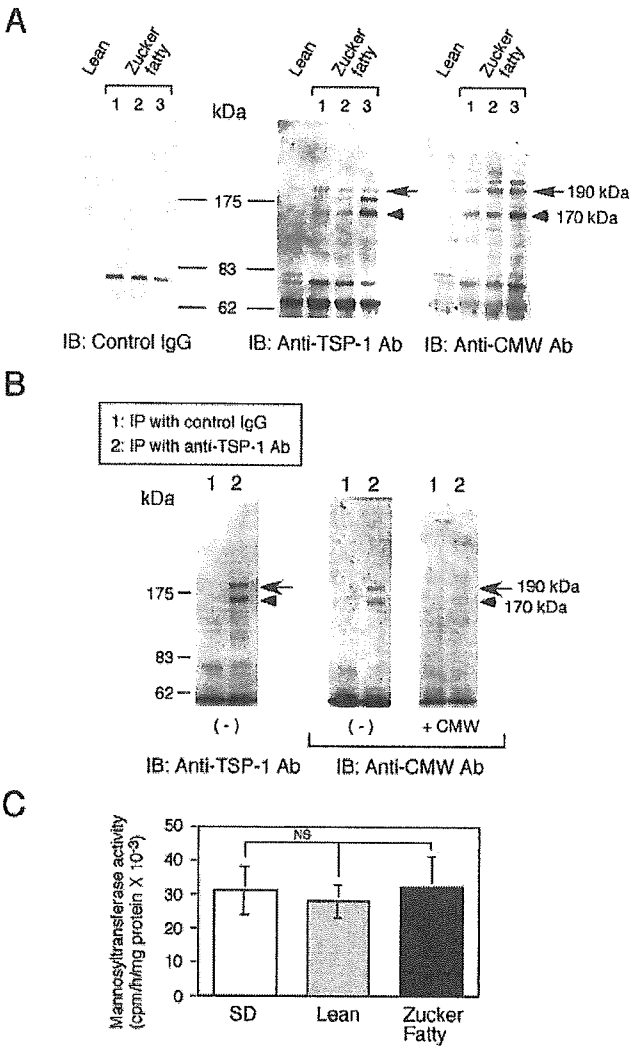

Fig. 8. C-mannosylated TSP-1 is accumulated in the aortic vessel of diabetic Zucker rats. (**A**) Tissue homogenates were prepared from aortic vessels of Zucker fatty (#1, #2, #3) and lean rats (20 weeks old) as described in *Materials and methods*. The samples were separated with 7.5% SDS–PAGE, and then immunoblot analysis was performed with the antibodies against TSP-1 and CMW. Both antibodies are immunoreactive to the bands of 190 kDa (arrows) and 170 kDa (arrowheads). The results represent three independent experiments. (**B**) TSP-1 was isolated from the aortic lysates of the Zucker fatty rat (#2) by immunoprecipitation using the anti-TSP-1 antibody. Normal rabbit IgG was also used for the control immunoprecipitation. The immunoprecipitates were examined by immunoblot analysis using the antibodies against TSP-1 and CMW after the separation with 5% SDS–PAGE. To confirm the specificity of the antibody, the membrane was incubated with the anti-CMW antibody in the presence or absence of 1 mM CMW (right). The results represent two independent experiments. (**C**) The C-mannosyltransferase activity was assayed with aortic tissue samples. The tissue homogenates were prepared from aortic vessels of Zucker fatty and lean rats (20 weeks old) as described in the methods. The samples from Sprague Dawley (SD) rats (20 weeks old) were also used for controls along with those of Zucker fatty rats. The data represent the mean ± SD of three or four independent experiments. NS, not significant (Bonferroni correction).

complications of blood vessels in diabetes. On the other hand, TSP-1 has been reported as a target of C-mannosylation (Hofsteenge *et al.*, 2001). Therefore, to investigate whether the expression of TSP-1 correlates with C-mannosylation, we also examined the expression of TSP-1 in the aortic vessel wall of Zucker fatty and lean rats. The expression of TSP-1 was elevated in the aortic vessel wall of Zucker fatty rats compared to lean rats.(Figure 7), consistent with previous findings (Stenina *et al.*, 2003). The levels of TSP-1 expression and protein C-mannosylation in the aortic tissues were also compared by immunoblot analysis between Zucker fatty and lean rats using each specific antibody (Figure 8A). The results showed that for both antibodies, the intensity of immunoreactive bands was significantly elevated in the aortic tissue of Zucker fatty rats compared to that of lean rats. Notably, the specific bands of 190 and 170 kDa were likely to be identical between the immunoblots for CMW and TSP-1. To investigate whether TSP-1 is C-mannosylated in the aortic tissues of Zucker fatty rats, it was immunoprecipitated with the anti-TSP-1

antibody from the aortic tissue lysates of Zucker fatty rats, and then the immunoprecipitates were examined by immunoblotting using the anti-CMW antibody. As shown in Figure 8B, the immunoprecipitated TSP-1 corresponded to the bands of 190 and 170 kDa. These bands were also reactive with the anti-CMW antibody. Furthermore, the intensity of these bands was diminished in the presence of free CMW (1 mM). Together, these results indicate that TSP-1 was C-mannosylated in the aortic tissues of Zucker fatty rats.

Next, the C-mannosyltransferase activity was examined in tissue homogenates from the aorta of Zucker fatty and lean rats. For comparison, the aortic tissues from Sprague Dawley rats were also examined. As shown in Figure 8C, there was no significant difference in the C-mannosyltransferase activity observed in the tissue homogenates from Sprague Dawley and Zucker fatty and lean rats, despite the fact that the C-mannosylation was apparently increased in the aortic tissues of hyperglycemic Zucker fatty rats (Figure 7). Therefore, C-mannosylation occurred on TSP-1, and the increased expression of C-mannosylated protein was highly correlated with that of target proteins such as TSP-1 in the aortic vessel wall of Zucker fatty rats.

Discussion

Although a wide variety of metabolic pathways are influenced by the pathological process of diabetes mellitus, enzymatic glycosylation in proteins is also altered in diabetes (Bar-On *et al.*, 1997; Berry *et al.*, 1980; Sharma *et al.*, 1987; Spiro and Spiro, 1971; Tepperman *et al.*, 1983). Changes in O-glycans have been described in renal tissues of alloxan diabetic rats (Spiro and Spiro, 1971). N-glycans in membrane or secretory proteins and dolichol metabolism were also altered in liver from streptozotocin-induced diabetic rats (Bar-On *et al.*, 1997; Berry *et al.*, 1980; Sharma *et al.*, 1987; Tepperman *et al.*, 1983). Despite reports concerning glycosylation in diabetes, not much is known about the pathophysiological significance of the diabetes-induced alteration of glycosylation metabolism, with a few exceptions, such as the core 2 GlcNAc structure in O-glycans and O-GlcNAc modifications.

Core 2 GlcNAc transferase is a glycosyltransferase involved in the biosynthesis of O-glycan, and its up-regulation is implicated in the pathogenesis of diabetic complications (Nishio *et al.*, 1995). The gene for core 2 GlcNAc transferase has been identified as being specifically up-regulated in rat diabetic cardiomyocytes (Nishio *et al.*, 1995). The up-regulation of core 2 GlcNAc transferase has been reported to enhance the actions of cytokines and induce a hypertrophic myocardium in transgenic mice, suggesting that specific changes to O-glycans have functional relevance in the pathogenesis of diabetic complications (Koya *et al.*, 1999). Furthermore, it has been reported that protein kinase C–dependent phosphorylation of core 2 GlcNAc transferase might be involved in the pathogenesis of diabetic retinopathy by mediating the increase in leukocyte–endothelial cell adhesion and capillary occlusion (Chibber *et al.*, 2003). On the other hand, O-GlcNAc modification is a unique form of monoglycosylation of Ser or Thr residues in proteins and is also influenced by hyperglycemic conditions in vivo and in vitro (Hanover, 2001; Parker *et al.*, 2004; Zachara and Hart, 2004). An increase in the modification of O-GlcNAc was observed in pancreatic β-cells of rats with streptozotocin-induced diabetes (Akimoto *et al.*, 2000; Hanover *et al.*, 1999; Liu *et al.*, 2000), rat aortic smooth muscle cells treated with high glucose (Akimoto *et al.*, 2001), and neonatal rat cardiomyocytes treated with high glucose (Clark *et al.*, 2003). In transgenic mice that overexpress O-GlcNAc transferase in adipose tissues and cardiac and skeletal muscles, insulin resistance and hyperleptinemia were induced (McClain *et al.*, 2002). In 3T3-L1 adipocytes, increased modification of O-GlcNAc by the inhibitor of N-acetylglucosaminidase resulted in insulin resistance associated with defects in protein kinase B/Akt activation (Vosseller *et al.*, 2002). Together, these results suggest a causative role for O-GlcNAc modifications in the development of insulin resistance and diabetic complications.

In contrast, it is not known whether hyperglycemia influences protein C-mannosylation. In the present study, we found that the level of C-mannosylation was elevated under hyperglycemic conditions in some cultured cells and diabetic tissues. In macrophage-like RAW264.7 cells, C-mannosylation was increased by hyperglycemic conditions, and the increase was concomitant with an increase in C-mannosyltransferase activity, suggesting that the promotion of C-mannosylation is due to the activation of C-mannosyltransferase under hyperglycemic conditions. We also examined whether C-mannosylation is induced by hyperglycemic conditions in other cell types such as Madin-Darby canine kidney cells. However, the up-regulation of protein C-mannosylation and C-mannosyltransferase activity was not observed in these cells cultured with a high glucose concentration (data not shown), suggesting that the up-regulation of C-mannosylation may not be common to all kinds of cells treated with high glucose. In RAW264.7 cells, the intracellular distribution of C-mannosylated proteins showed a perinuclear vesicular pattern, and was similar to that of clathrin heavy chain, a marker expressed in secretory vesicles and the trans-Golgi network. This strongly suggests that C-mannosylated proteins are part of the secretory pathway. The localization is also consistent with findings that C-mannosylated proteins are mainly secretory or membrane proteins, such as compliments, cytokines, and cytokine receptors (Furmanek and Hofsteenge, 2000).

The effect of hyperglycemic conditions on C-mannosylation was also examined in tissues of the Zucker fatty rat, a diabetic animal model. We found that protein C-mannosylation was specifically increased in the aortic tissues of Zucker fatty rats. However, there was no significant increase of C-mannosyltransferase activity in aortic tissue homogenates from Zucker fatty rats compared with controls. These results suggest that the increase of C-mannosylation in the diabetic aorta is not simply explained by the up-regulation of C-mannosyltransferase activity. Other possible explanations for the increase in C-mannosylation could be an increase in the synthesis of dolichol-P-mannose, a donor substrate for C-mannosylation (Doucey *et al.*, 2000) or that of target proteins bearing the Trp-X-X-Trp motif. Sharma *et al.* (1987) reported that production of dolichol-P-mannose and dolichol-P-oligosaccharide was significantly down-regulated in liver

slices from streptozotocin-treated diabetic rats. In contrast, an increase in the concentration of dolichol was observed in diabetic liver tissues of streptozotocin-treated rats, which suggests a dolichol-mediated enhancement of protein N-glycosylation by hyperglycemia (Bar-On *et al.*, 1997). Although it was not clear why conflicting results were obtained in the two studies concerning an altered dolichol metabolism in the liver of streptozotocin-treated rats, further investigation might be required to understand the correlation between C-mannosylation and the metabolism of dolichol in diabetic conditions.

To investigate the correlation between the levels of C-mannosylation and the expression of proteins targeted for C-mannosylation, we focused on the expression of TSP-1 in aortic tissues. TSPs are a family of multimeric, multidomain glycoproteins that function at the cell surface and in the extracellular matrix to regulate cell–cell interactions and cellular signaling through binding with integral molecules such as TGF-β, integrins, collagens, proteoglycans, CD36, CD47, calreticulin, and so forth (Adams, 2001; Elzie and Murphy-Ullrich, 2004; Lawler, 2000). TSP-1 is the best characterized of the TSPs, and its subunits are glycoylated with N-glycans (Furukawa *et al.*, 1989) and O-glycans (Hofsteenge *et al.*, 2001). TSP-1 is also C-mannosylated at the Trp-X-X-Trp motif in the TSP type 1 repeat (Hofsteenge *et al.*, 2001). In the present study, we found that TSP-1 was C-mannosylated in the aortic tissues of Zucker fatty rats, which was consistent with previous findings (Hofsteenge *et al.*, 2001). Furthermore, in immunohistochemical and immunoblot analyses, the levels for TSP-1 expression and protein C-mannosylation were concomitantly elevated in the aortic vessel of Zucker fatty rats compared to that of lean rats. Although the precise mechanism for the hyperglycemia-induced change of C-mannosylation is not yet clear, the different responses of C-mannosyltransferase activity seen in RAW264.7 cells and the aortic tissue of Zucker fatty rats suggest that the hyperglycemia-induced change of C-mannosylation is regulated differently in different types of cells or tissues. Collectively, the results obtained by using Zucker fatty rats suggest that the diabetes-induced increase of C-mannosylation in the aortic tissues is partly due to the diabetes-induced increase in the expression of target proteins such as TSP-1 to be C-mannosylated.

It has been reported that the expression of TSP-1 increased in aortic vessel walls of diabetic Zucker rats (Stenina *et al.*, 2003). In that study, the authors suggested a relation between increased TSP-1 expression and accelerated atherosclerosis in the vascular tissues because TSP-1 is known to function in a variety of biological events, such as cell attachment, cell proliferation, angiogenesis, and apoptosis. Their findings are consistent with the results obtained in the present study. Atherosclerosis is a major vascular complication in diabetes (Semenkovich and Heinecke, 1997), and the involvement of TSP-1 in the pathology of vascular impairment seems to be consistent with the high glucose–induced up-regulation of TSP-1 expression in renal mesangial cells (Holmes *et al.*, 1997; McGregor *et al.*, 1994; Murphy *et al.*, 1999; Poczatek *et al.*, 2000; Tada and Isogai, 1998; Wang *et al.*, 2003; Yevdokimova *et al.*, 2001) and renal tissues from Zucker fatty rats (Olson *et al.*, 1999).

In terms of the structural characteristics and functions of TSP-1, the Trp-X-X-Trp motif of the TSP type 1 repeat is believed to play an important role in the binding of TSP-1 with molecules such as glycosaminoglycans, TGF-β, and matrix metalloproteases (Adams, 2001; Elzie and Murphy-Ullrich, 2004). In fact, a study of the crystal structure of the TSP-1 type 1 repeats revealed that the Trps in the structure are oriented so that their polar atoms are exposed and available for potential ligand binding (Tan *et al.*, 2002). On the other hand, the Trp-X-X-Trp motif has also been revealed to be specifically modified by C-mannosylation in the case of TSP-1, suggesting some functional regulation of TSP-1 by C-mannosylation (Hofteenge *et al.*, 2001; this study). Although how TSP-1 contributes to the diabetic complications is not well understood, the function of C-mannosylation may also need to be clarified to understand the functional regulation of TSP-1 in the pathogenesis.

Recently, chemically synthesized CMW and C-mannosylated peptides have become available for biomedical research (Manabe and Ito, 1999; Nishikawa *et al.*, 1999, 2001). These chemicals and the specific antibody against CMW generated in this study are powerful tools for further investigation of the biological functions of C-mannosylation and C-mannosylated proteins in the cell.

Materials and methods

Materials

The mouse monoclonal antibodies against TSP-1 (clone A6.1) and clathrin heavy chain (clone X22) were obtained from NeoMarkers and Affinity Bioreagents (Golden, CO), respectively. Dolichol-P-[6-^{3}H]mannose (40 Ci/mol) (ART791) was obtained from American Radiolabeled Chemicals (St. Louis, MO). The acceptor substrate peptide, N-AC-Lys-Pro-Pro-Gln-Phe-Ala-Trp-Ala-Gln-Trp-Phe-Glu-NH_2, was chemically synthesized at RIKEN (Saitama, Japan). The other reagents used in the study were of high-quality grade and from Sigma (St. Louis, MO) or Wako Pure Chemicals (Osaka, Japan).

Synthesis of CMW

The CMW derivative, Fmoc-C^2-α-D-C-mannosylpyranosyl-L-tryptophan, was synthesized as previously described (Manabe and Ito, 1999). The purity and identity of the final product were verified by ^{1}H nuclear magnetic resonance spectroscopy and matrix-assisted laser desorption ionization (MALDI) mass spectrometry. The protein chemical shifts and coupling constants are consistent with those reported before. The mass observed by MALDI mass spectrometry is consistent with the expected mass of the correct product.

Preparation with immunizing antigen

Fmoc-C^2-α-D-C-mannosylpyranosyl-L-tryptophan was conjugated with KLH or ovalbumin by 1-ethyl-3-[3-dimethylamino-propyl]carbodiimide hydrochloride using the Imject Immunogen conjugation kit (Pierce Biotechnology, Rockford, IL), according to the manufacturer's instructions. Fmoc was removed by alkaline treatment with 1 M sodium

hydroxide and neutralized with hydrochloride. The sample was then desalted with gel filtration using a NAP-10 column (Amersham Pharmacia Biosciences, Little Chalfont, U.K.) and used as the immunizing antigen.

Generation and affinity purification of antibodies

Rabbits were immunized with KLH conjugated with CMW, then polyclonal antisera were generated according to the conventional protocol (Sigel *et al.*, 1983). For affinity purification of the antibodies, CMW-conjugated affinity resins were prepared. The C-mannosylated peptide, C-Mannose-Trp-Ser-Pro-Trp-Cys, was synthesized as described before (Manabe and Ito, 1999). The peptide was conjugated through sulfhydryl residues of Cys with SulfoLink coupling agarose using a SulfoLink kit (Pierce) according to the manufacturer's directions. The antiserum was applied to the affinity resins and washed extensively with phosphate buffered saline (PBS, pH 7.2). The bound antibodies were eluted from the resins with 0.1 M glycine (pH 2.5), and neutralized by adding a 1/40 volume of 2 M Tris-hydrochloride (pH 8.5). The eluted solution was concentrated using a centricon (YM-10, Amicon) and then desalted with a gel filtration column equilibrated with PBS.

ELISA

One hundred microliters of a 2.5 μg/ml solution of ovalbumin conjugated with CMW in sodium carbonate buffer (pH 9.0) was added per well to a 96-well polystyrene microwell plate overnight at 4°C. The plate was washed with PBS and then blocked for 1 h with a 3% bovine serum albumin (BSA) in PBS. The wells were washed with PBS and incubated with 100 μl antibody solution for 2 h at room temperature. Then the wells were washed with PBS and incubated with horseradish peroxidase-conjugated anti-rabbit IgG (Dako, Copenhagen) for 1 h at room temperature. After four washes with PBS, the wells were developed with a peroxidase substrate, TMB one solution (Promega, Madison, WI), and the absorbance at 450 nm was measured in a microplate reader.

Immunoblot analysis

Cultured cells were harvested and lysed in lysis buffer (20 mM Tris-hydrochloride [pH 7.2], 150 mM sodium chloride, and 1% Triton X-100 including protease inhibitors [20 μM APMSF, 50 μM pepstatin, 50 μM leupeptin]). After centrifugation at 8000 × *g* for 20 min, the supernatants were collected and used for the following assay. Protein samples were subjected to 5, 7.5, or 10% sodium dodecyl sulfate–polyacrylamide gel electrophoresis (SDS–PAGE) under reducing conditions and then transferred to a nitrocellulose membrane as described elsewhere (Ihara *et al.*, 1997). The membrane was blocked with 5% skim milk in Tris-buffered saline (10 mM Tris-hydrochloride [pH 7.2] and 150 mM sodium chloride) and then incubated at 4°C overnight with the primary antibody in the blocking buffer. The blots were coupled with the peroxidase-conjugated secondary antibodies, washed, and then developed using the ECL chemiluminescence detection kit (Amersham Pharmacia Biosciences) according to the manufacturer's instructions.

Cell culture

RAW264.7 cells were obtained from American Type Culture Collection. Cells were cultured in Dulbecco's modified Eagle's medium containing 5.5 mM glucose, supplemented with 10% fetal calf serum under a humidified atmosphere of 95% air and 5% CO_2 at 37°C. For hyperglycemic condition, the cells were cultured in Dulbecco's modified Eagle's medium containing 30 mM glucose for more than 5 days.

Fluorescence microscopy

Cells (5×10^4/ml) were grown on Lab-Tek chamber slides (Nunc, Roskilde, Denmark) for 24 h. They were fixed with 4% paraformaldehyde in PBS and permeabilized for 10 min with PBS containing 1% Triton X-100. The cells were then blocked with 1% BSA in PBS, incubated with the antibody for 1 h, and washed with PBS containing 1% BSA. The immunoreactive primary antibodies were visualized with fluorescein isothiocyanate (FITC)-conjugated anti-rabbit immunoglobulins (Cappel, Aurora, OH) or rhodamine-conjugated anti-mouse immunoglobulins (Dako). After a wash, the stained cells were mounted in the Vectashield medium. A Zeiss Axioskop2 (Carl Zeiss, Jena, Germanny), with epi-illumination for fluorescence, was used for the fluorescence microscopic analysis.

Assay of C-mannosyltransferase activity

The C-mannosyltransferase activity was assayed according to the methods of Doucey *et al.* (1998) with a slight modification. Enzyme assays with cell extracts were carried out in a 25 μl reaction volume containing 20 mM HEPES (pH 7.2), 110 mM potassium acetate, 2 mM magnesium acetate, 0.2% TritonX-100, 6.25 nmol of dolichol-P-[6-^{3}H]mannose (40 Ci/mmol), and 0.9 mM of the substrate peptide for 2 h at 37°C. The reaction was stopped by adding 2 ml chloroform/methanol (3/2, vol/vol) and 0.48 ml water. After centrifugation, 0.2 ml of the upper phase containing the peptide was collected and then subjected to scintillation counting to determine the radioactivity.

Animals

Sprague Dawley, Zucker diabetic fatty (fa/fa), and lean (fa/+) rats were obtained from the Charles River Laboratory (Japan) and fed and housed in standard conditions at 22°C. The male rats at 20 weeks old were used for the experiments. Use of the animals was authorized according to the guidelines of the Declaration of Helsinki and the principles for the care and use of animals (Committee on Care and Use of Laboratory Animals of the Laboratory Animals Resources Commission on Life Sciences National Research Council [1985]. Guide for the Care and Use of Laboratory Animals, Public Health Service National Institutes of Health NIH Publication No. 86-23, Bethesda, MD).

Immunohistochemistry of rat aortic vessels

Tissues were embedded into paraffin, and sections were stained with the antibodies against cMW and TSP-1. Immunoreactive signals of primary antibodies were visualized with diaminobenzidine chromogenic substrate as described